TAMPEREEN TEKNILLINEN YLIOPISTO
TAMPERE UNIVERSITY OF TECHNOLOGY

ESSI TERVOLA

CHARACTERIZATION OF CARBAZOLE DERIVATIVES AND MODULATION OF THEIR LUMINESCENCE

Master of Science thesis

Examiners:
Prof. Arri Priimägi
D. Sc. (Tech.) Tero-Petri Ruoko
Examiner and topic approved by the
Faculty Council of the Faculty of
Natural Sciences
12.12.2018

ABSTRACT

ESSI TERVOLA: Characterization of carbazole derivatives and modulation of their luminescence
Tampere University of Technology
Master of Science thesis, 59 pages, 5 Appendix pages
December 2018
Master's Degree Program in Engineering and Natural Sciences Technology
Major: Chemistry
Examiners: Prof. Arri Priimägi, D. Sc. (Tech.) Tero-Petri Ruoko
Keywords: carbazole, fluorescence spectroscopy, non-covalent bonding, intermolecular interactions

This thesis investigates the effects of intermolecular interactions such as hydrogen bonding, halogen bonding and ionic interactions on the emission of organic compounds in solution and solid state. The study focuses on carbazole derivatives with either hydrogen or halogen bond acceptor and donor moieties. These non-covalent bond donors and acceptors are characterized using absorption and emission spectroscopy as well as time-correlated single photon counting. In the solid state, the films are also characterized using optical profilometry and digital holographic microscopy.

Titration series using pentafluoroiodobenzene, phenol, benzenesulfonic acid and pyridine are prepared to study the emission modulation induced by the non-covalent bonding. In addition to emission spectra, the changes in the excited-state lifetime and emission quantum yields are determined. The effects of non-covalent bonding in the solid state are studied forming polymer-chromophore complexes capable of weak interactions. Polystyrene is used as a reference polymer, poly(vinyl phenol) as a hydrogen bond donor, poly(4-vinyl pyridine) as a halogen bond acceptor, and finally poly(styrenesulfonic acid) in the formation of ionic interactions.

Halogen bonding in solution induces intramolecular charge transfer that modulates the emission of the compound. The emission modulation results in increased emission intensity and a blue-shift in the emission spectra. Even greater effects can be seen with ionic interactions using benzenesulfonic acid which enhances the emission intensity and emission quantum yield up to 0.93. Weak hydrogen bonding did not result in emission modulation. Halogen bonding in solution was also studied using carbazole derivatives as halogen bond donors, but carbazole derivatives displayed greater potential as halogen bond acceptors than donors. Similar effects were also observed in the solid state, only in less significant amounts.

TIIVISTELMÄ

ESSI TERVOLA: Karbatsolijohdannaisten luminesenssin modulaatio ja karakterisointi
Tampereen teknillinen yliopisto
Diplomityö, 59 sivua, 5 liitesivua
Joulukuu 2018
Teknis-luonnontieteellinen koulutusohjelma
Pääaine: Kemia
Tarkastajat: Prof. Arri Priimägi, TkT Tero-Petri Ruoko
Avainsanat: karbasoli, fluoresenssispektroskopia, ei-kovalentit sidokset, molekyylien väliset vuorovaikutukset

Tässä diplomityössä perehdytään molekyylien välisten vuorovaikutusten, kuten vety- ja halogeeni- sekä ionisidoksen tutkimiseen liuoksessa ja kiinteässä olomuodossa. Tutkimus keskittyy karbatsolijohdannaisiin, jotka voivat toimia vety- ja halogeenisidoksen vastaanottajina tai luovuttajina. Heikkojen sidosten vastaanottaja- ja luovuttajamolekyylejä karakterisoidaan absorptio- ja emissiospektroskopian avulla sekä Time Correlated Single Photon Counting -menetelmän avulla. Filmejä karakterisoidaan myös optisella profilometrilla ja digitaalisella holografiamikroskoopilla.

Heikkojen vuorovaikutusten indusoimaa emissiomodulaatiota liuoksessa tutkitaan useilla titraatiosarjoilla. Emissiospektrin lisäksi määritetään viritystilan elinikä ja emission kvanttisaanto. Heikkojen vuorovaikutusten aikaansaamia vaikutuksia kiinteässä olomuodossa tutkitaan muodostamalla polymeeri-kromofori komplekseja, jotka muodostavat keskenään heikkoja vuorovaikutuksia. Polystyreeniä käytetään referenssimateriaalina, poly(vinyylifenolia) vetysidoksen luovuttajana, poly(4-vinyylipyridiiniä) halogeenisidoksen vastaanottajana ja poly(styreenisulfonihappoa) ionisten vuorovaikutusten muodostamisessa.

Halogeenisidos liuoksessa aiheuttaa intramolekulaarista varauksen siirtoa, joka muuttaa yhdisteen emissiota. Emission modulaatio johtaa suurempaan emission intensiteettiin ja sinisiirtymään emissiospektrissä. Yhä suuremmat vaikutukset voidaan havaita käyttämällä bentseenisulfonihappoa. Ioniset vuorovaikutukset kasvattavat yhdisteen emission intensiteettiä ja emission kvanttisaantoa jopa 0.93 saakka. Heikot vetysidokset eivät vaikuttaneet yhdisteen emission intensiteettiin. Halogeenisitoutumista liuoksessa tutkittiin myös käyttämällä karbatsolijohdannaista halogeenisidoksen vastaanottajana, mutta muodostuneet sidokset olivat liian heikkoja aiheuttaakseen merkittäviä muutoksia yhdisteen emissiossa. Samankaltaisia tuloksia havaittiin myös kiinteässä olomuodossa, mutta pienemmissä määrin.

PREFACE

This thesis was conducted in the Laboratory of Chemistry and Bioengineering at Tampere University of Technology from May to December in 2018. First, I would like to thank my supervisor Arri Priimägi for giving me the opportunity to join the Smart Photonic Materials group and for the concept for this work. I would also like to express my gratitude to Tero-Petri Ruoko for his continuous guidance and support throughout this work.

I would like to thank Jagadish Salunke for the synthesis of the molecules studied in this thesis as well as Nikita Durandin for his help with various equipment in the laboratory. Lastly, I would like to thank the whole Smart Photonic Materials group for welcoming me into their midst and making this a pleasant journey.

Finally, I would like to thank my fiancé Jussi for his loving support during my studies.

Jyväskylä, 29th November, 2018

Essi Tervola

CONTENTS

LIST OF ABBREVIATIONS AND SYMBOLS

ϵ	Molar absorption coefficient
λ	Wavelength
λ_{em}	Emission wavelength
λ_{ex}	Excitation wavelength
λ_{max}	Wavelength of the emission maximum
ϕ	Quantum yield
$\phi(x, y)$	Phase shift
τ	Excited-state lifetime
A	Absorbance
BSA	Benzenesulfonic acid
c	Concentration
c_0	The speed of light
CFD	Constant fraction discriminator
DCM	Dichloromethane
DHM	Digital holographic microscope
DMF	Dimethylformamide
DPA	9,10-Diphenylanthracene
e	Napier's constant
E	Energy
FTIR	Fourier transform infrared spectroscopy
h	Plank's constant
$h(x, y)$	Height
HB	Hydrogen bond
HOMO	Highest occupied molecular orbital
I	Intensity of light
IC	Internal conversion
ICT	Internal charge transfer
IR	Infrared
IRF	Instrument response function
ISC	Intersystem crossing
IUPAC	The International Union of Pure and Applied Chemistry
l	Length
LE	Locally excited state
M	Mirror
MCA	Multichannel analyzer
n	Refractive index

OLEDs	Organic light-emitting diodes
PD	Photodiode
PFIB	Pentafluoroiodobenzene
PMT	Photomultiplier tube
PS	Polystyrene
PSS	Poly(styrenesulfonic acid)
PVPh	Poly(vinyl phenol)
P4VP	Poly(4-vinylpyridine)
QY	Quantum yield
$R(\lambda)$	The ratio of voltages from sample and reference chamber without the sample in TCSPC measurements
$S(\lambda)$	The ratio of voltages from sample and reference chamber with the sample in TCSPC measurements
r(t)	Instrument response function
S_0	Electronic ground state of a molecule
S_1	First singlet excited state of a molecule
S_a	Roughness average of the surface
S_q	Root mean square of the surface roughness
S_{ku}	Kurtosis of the surface
S_{sk}	The skewness of the surface
SD	Synchronous detector
s(t)	Sample response function
t	Time
T	Transmission
T_1	First triplet excited state of a molecule
TAC	Time-to-amplitude converter
TCSPC	Time correlated single photon counting
TDDFT	Time-dependent density functional theory
THF	Tetrahydrofuran
U	Voltage
UV	Ultraviolet
VR	Vibrational relaxation
XB	Halogen bond

1. INTRODUCTION

The absorption of a photon is one of the most common chemical reactions that occur. The absorbed energy is released as heat or as an emission of a photon. Organic luminescent materials are key components in many applications that range from organic light emitting diodes (OLEDs) to fluorescence probes for example. [1, 2] The search for highly efficient blue-light emitting materials is still a timely issue for improving the efficiencies of organic light-emitting diodes for various technologies. Carbazoles are highly emitting materials commonly used in blue-light emitting devices. This Thesis is focused on characterization of the luminescence properties of various carbazole derivatives and their emission modulation.

Emission properties are characteristic to a compound depending on the emitting moiety of the molecule. In this Thesis, the emission properties of carbazole derivatives are tuned through forming intermolecular interactions. Hydrogen bonding, despite being a weak interaction, has proved its importance in many biological systems and is perhaps the most well-known non-covalent bond. Extremely strong hydrogen bond donors can also be used to protonate the acceptor molecule and the formation of a salt can affect the luminescence of the system. In addition to that, halogen bonding as risen as a competitive alternative to hydrogen bond, and is perhaps even more prominent than hydrogen bond. [3] The weak interactions in light-emitting compounds could provide a path to tunable light-emitting devices by controlling the non-covalent bonding in the system. Moreover, non-covalent bonding provides the means to exploit self-assembly and to avoid intricate synthesis routes.

The carbazole core is highly electron dense and with different substituents, good non-covalent bond donors and acceptors could be designed. Here, a pyridyl group is added to benzophenone-carbazole to weaken the electron donating nature of the carbazole core and to induce the formation of the non-covalent bond. Non-covalent bond acceptors are studied with iodine derivatives of benzophenone-carbazole. The samples are characterized using absorption and emission spectroscopy. Also, the emission properties of the materials are described by determining the excited-state lifetimes using Time Correlated Single Photon Counting (TCSPC) and by their emission quantum yields.

This thesis studies the supramolecular interactions between the molecular components to further understand the possibilities in the modulation of the emission properties of the emitters. The non-covalent bonding is first studied in solution and further in the solid state. Chapter 2 consists of the theoretical background needed to comprehend the supramolecular and photochemistry behind the results of the experiments. The materials used in the experiments as well as the instrumentation are introduced in chapter 3. Chapter 3 also explains the execution of the experiments. Chapter 4 presents the results and discussion of the experiments, and is composed of the solution and solid-state studies. The solid-state studies also include topological and stability studies of some of the compounds. Finally, the results are summarized in the conclusions given in chapter 5.

2. THEORETICAL BACKGROUND

This chapter introduces the essential concepts needed to understand the chemistry behind the results of this thesis. Subjects covered in this chapter include absorption, emission, and intermolecular interactions. It also introduces the reader to polymers as optical materials.

2.1 Interactions of photons with matter

When incident light hits matter the photons interact with it and excite the molecule. The excited state spontaneously relaxes to the ground state using either non-radiative or radiative relaxation route. This is the basis of absorption and emission of light. These interactions are further described in this section.

2.1.1 Absorption

Absorption is a photon-assisted transition between two energy levels. It occurs when a photon of appropriate energy is absorbed by a molecule, which induces an electronic transition to a higher energy level. The energy absorbed is inversely proportional to the wavelength of the incident light [4]

$$\Delta E = \frac{hc_0}{\lambda} \tag{2.1}$$

where E is energy, h is Planck's constant, c_0 is the speed of light and λ is wavelength. When a sample is irradiated with light, it absorbs energy according to Lambert-Beer's law: [5]

$$log(\frac{I}{I_0}) = -\varepsilon lc \tag{2.2}$$

where I_o is the intensity of the light entering the absorbing medium, I is the intensity of the light leaving the absorbing medium, ε is the molar absorption coefficient, l is

the length of the path in which energy is absorbed and c is the concentration of the absorbing species. The logarithmic ratio of the light intensities before and after the sample can also be expressed in another form of the Lambert-Beer's law

$$A = \varepsilon l c \tag{2.3}$$

where A is the absorbance of the sample. The molar absorption coefficient can be used to describe the strength of the electronic transition. [5] It expresses the ability of a molecule to absorb light of certain wavelength in a given solvent. A high molar absorption coefficient implies that an electronic transition is very probable. The light absorbing part of the molecule is called a chromophore. [6] It is a chemical moiety which absorbs radiation at nearly the same wavelength in different molecules. [5]

2.1.2 Electronic transitions

Atoms are linked by either σ or π bonds depending on the nature of the bond. In addition to those, a molecule may possess non-bonding electrons, which are referred to as lone electron pairs. These orbitals are denoted by the letter n. The absorption of a photon can result in many electronic transitions depending on the energy of the absorbed photon. A transition from the π orbital to the antibonding π orbital is denoted by $\pi \rightarrow \pi^*$. Transitions from the ground state to the excited states are generally classified according to the energy that is needed for the transition: [6]

$$n \rightarrow \pi^* < \pi \rightarrow \pi^* < n \rightarrow \sigma^* < \sigma \rightarrow \pi^* < \sigma \rightarrow \sigma^*$$

A $\pi \rightarrow \pi^*$ transition requires the molecule to have double or triple bonds, whereas $n \rightarrow \pi^*$ transitions require both double or triple bonds and non-bonding electron pairs. These transitions are typical for carbonyl and azo groups. [6] The highest occupied molecular orbital (HOMO) is the highest electronic state in energy, which has electrons on it, whereas, the lowest unoccupied molecular orbital (LUMO) is the molecular orbital lowest in energy without any electrons. These are defined for a molecule in the ground-state. Thus, the lowest energy transition for a molecule in the ground-state will be the transition from HOMO to LUMO. [4]

An electronic transition in a polyatomic molecule can result in many vibrational or rotational transitions. These transitions occur at similar energies which leads

to overlapping and broad absorption bands in UV-visible absorption spectra. The energy difference between the initial and final electronic states of the transition determines the frequency of the spectral line. To a certain approximation, the absorption spectrum of a molecule can be thought of as a sum of the absorption spectra of the chromophores within the molecule. [5]

2.1.3 Excited-state relaxation routes

The relaxation route from an excited state depends on the rates of a number of competing processes. The excited state can return to the ground state via radiative or non-radiative decay. [6] There are two main selection rules for electronic transitions induced by a photon; spin-forbidden transitions and symmetry-forbidden transitions. According to the spin selection, when an electron from the ground state is excited to a higher electronic state, its spin is unchanged, meaning that $\Delta S = 0$. Spin multiplicity can be specified from the total spin, S, so that spin multiplicity $= 2S + 1$. [4] A singlet state is denoted by spin multiplicity 1, whereas a triplet state is denoted by spin multiplicity 3. The triplet state is called such, since is represents three separate states that are all equal in energy. [6]

The ground state of a molecule is usually a singlet state, whereas an excited state can be either a singlet or triplet state. The excited state can also have multiple vibrational states. When a photon is absorbed it initiates an electronic transition from the ground state S_0 to usually one of the excited vibrational states of the first excited-state S_1. The electron quickly relaxes to the lowest vibrational state of S_1. This process is called vibrational relaxation (VR). It is a non-radiative process which occurs due to thermal collisions in the system. In a non-radiative process, the energy is lost as heat to the surroundings. [5] Vibrational relaxation always occurs between vibrationally excited states and the vibrational ground state within a given electronic state. This is a rapid process and occurs within $10^{-13} - 10^{-9}$ s. [4]

The different routes of relaxation of the excited state are often represented by a Jablonski diagram, which is depicted in Figure 2.1 and further discussed in the following sections.

Internal conversion and fluorescence

Internal conversion (IC) is a non-radiative process in which a higher excited electronic state S_2, S_3 etc. relaxes to the lowest excited electronic state S_1. The energy difference between higher excited electronic states is relatively small, and therefore

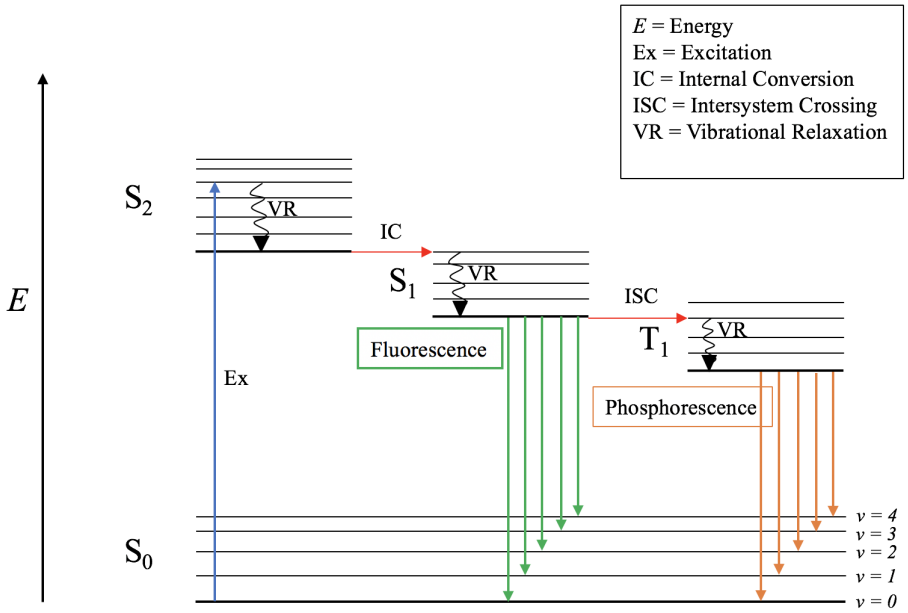

Figure 2.1 *Jablonski diagram of various excited-state relaxation routes.*

there is a high probability that vibrational states belonging to different electronic states are very close in energy. Because of this, internal conversion is a rapid process and the system is always relaxed to the lowest excited electronic state before fluorescence occurs. Internal conversion between excited states occurs within $10^{-14} - 10^{-11}$ s and always occurs between two states with the same multiplicity. [4, 6]

Fluorescence is the emission of a photon when the system relaxes from an excited state to the ground state. A substance that emits light upon excitation is called a fluorophore [1]. Internal conversion happens at a much higher rate than fluorescence and according to Kasha's rule, fluorescence from organic compounds usually originates from the lowest vibrational state of the lowest excited singlet state. Exceptions to Kasha's rule may occur with samples that have exceptionally large energy gap between the first and second excited singlet state. [4] Vibrational relaxation to the lowest vibrational state prior to emission results in losing some of the absorbed energy in the process. For this reason, the fluorescence spectrum is always located at higher wavelengths than the absorption spectrum. The fluorescence spectrum forms a mirror-image of the absorption spectrum only if the ground state and excited state are similar in geometries. Apart from a few exceptions, fluorescence always occurs from S_1 to the ground state and is independent on excitation wavelength. [6]

One of the possible routes of relaxation of the excited state is delayed fluorescence. It is generally described by two mechanisms. P-type delayed fluorescence is also called

triplet-triplet annihilation. [7] Essentially, the interaction of two molecules in the triplet state produces one molecule in the ground state and one in the first excited state. The result is two species, one with emission at a normal fluorescence rate and another with an emission rate half of that of phosphorescence. E-type delayed fluorescence is initiated by thermal activation, in which the first excited singlet state becomes populated by electrons from the first excited triplet state. [4, 8]

Intersystem crossing and phosphorescence

Although excitation from a singlet state to a triplet state is a spin-forbidden transition and does not occur, the triplet state can be accessed after excitation to a singlet state. A molecule can undergo a conversion where the spin multiplicity of the promoted electron is changed. This is called intersystem crossing (ISC) and it occurs from an excited singlet state to the triplet state. [5] Intersystem crossing can be fast enough to compete with other relaxation routes. [6]

Electronic transitions from a singlet state to a triplet state are forbidden. However, there is always a weak interaction between states with different multiplicities due to spin-orbit coupling, which enables intersystem crossing. The orbital motion of an electron produces a magnetic field, which interacts with the electron spin and causes spin-orbit coupling. The efficiency of spin-orbit coupling depends linearly with the fourth power of the atomic number. Therefore, heavier atoms are more likely to experience intersystem crossing. This is also called the "heavy atom effect". [9] Thus, incorporating a heavy atom in a molecule can enhance the $S_1 \rightarrow T_1$ transition probability. Intersystem crossing is also more probable between symmetric singlet and triplet states. Similar geometry occurs when the singlet state S_1 has the same energy as one of the excited vibrational states of the T_1 triplet state. [6] The efficiency of intersystem crossing is thus determined by the energy gap between the singlet and triplet states. [4]

The wavelength difference between the first absorption maximum and the maximum of fluorescence is called the Stokes shift. [6] It represents the energy difference lost in the internal conversion. In general, the T_1 excited state is lower in energy than the S_1 excited state. This obeys Hund's rule since electrons in a triplet state have parallel spin and therefore minimum energy repulsion. [4] This results in a further shift to higher wavelengths in the phosphorescence spectrum compared to the fluorescence spectrum. An example of electronic transitions in a spectrum and the Stokes shift is depicted in Figure 2.2. A shift to higher wavelengths in spectrum is also referred to as a red-shift. Due to longer lifetime, phosphorescent materials have considerably

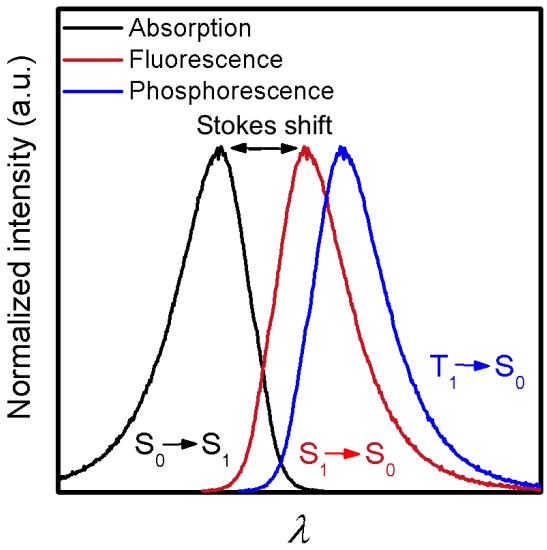

Figure 2.2 *A general example of absorption, fluorescence and phosphorescence spectra and their relation to each other.*

wider possibilities than their fluorescent counterparts and are desired materials for optical devices because of the possibility to harness three times more energy from the triplet excitons. [2]

Quantum yield and lifetime

Excited molecules stay in the S_1 electronic state a certain time before undergoing one of the relaxation routes. During this time, fluorescence decreases exponentially reflecting the average lifetime of the molecules in the S_1 state. [6] For organic molecules, the lifetime of the excited S_1 state can range from tens of picoseconds to hundreds of nanoseconds. Fluorescence is an allowed transition and therefore the lifetime is usually quite short, typically less than 10^{-7} s. Triplet states, however, have much longer lifetimes since phosphorescence is due to a forbidden transition. Phosphorescence lifetimes usually range from microseconds to seconds. [6] The lifetime τ of the excited state is given by the time in which the concentration of the excited state decreases to $1/e$ of its original value. [4] The excited state lifetime can be determined using time-resolved fluorescence spectroscopy methods, such as TCSPC, which is further described in section 3.1.

The emission quantum yield ϕ can be defined as the ratio between the number of photons emitted from the S_1 excited state and the number of absorbed photons by the ground state. [4] It can be determined by integrating the area under the emission

spectrum and comparing it to a reference with a known emission quantum yield. This must be done with very dilute solutions to avoid inner filter effects and ensure a linear response on the intensity. High concentration causes the excitation light to be absorbed only on the surface of the sample. This results in spectral distortions due to inhomogeneous excitation. The quantum yield (QY) of the substance can be calculated using equation (2.4). [1]

$$\phi = \phi_{ref} \frac{I}{I_{ref}} \frac{A_{ref}}{A} \frac{n^2}{{n_{ref}}^2} \tag{2.4}$$

where I is the integrated intensity of the emission spectrum, A is the absorbance at the excitation wavelength and n is the refractive index of the solvent used. [1] When a molecule is excited, usually a number of competing processes occur and fluorescence is only one of them. The fluorescence quantum yield is dependent on these other processes in such a way that

$$\phi_f + \phi_{\mathrm{ISC}} + \phi_{\mathrm{IC}} = 1 \tag{2.5}$$

where ϕ_f is the quantum yield of fluorescence, ϕ_{ISC} is the quantum yield of intersystem crossing, and ϕ_{IC} is the quantum yield of internal conversion. The fluorescence quantum yield is always between 0 and 1, 1 meaning that all absorbed photons are emitted as fluorescence. [4]

Fluorescence quenching

The relaxation of an excited state by intermolecular interactions is referred to as quenching. This can be due to other absorber molecules or solvent molecules in the surroundings, for example. One of the most common fluorescence quenchers is molecular oxygen. [4] Oxygen causes fluorescence quenching, but its effect on the quantum yields and lifetimes depends on the compound and the surrounding medium. Generally quantum yields can be increased by lowering the temperature and thereby reducing the non-radiative relaxations induced by thermal collisions.

Room temperature phosphorescence of organic molecules can be diminished by collisions with oxygen, solvent molecules or impurities. [6] Due to the longer lifetimes, phosphorescence is more susceptible to quenching than fluorescence and it is not usually observed in room temperature solutions. [4] Usually, phosphorescence needs to be enhanced by other methods, such as lowering the temperature or rigid matrices.

2.2 Intermolecular interactions

Intermolecular interactions are induced by intermolecular forces between different molecules, that can be both attractive and repulsive forces. Intermolecular interactions include dipole-dipole interactions, including hydrogen and halogen bonding, ionic interactions and London-dispersion forces. They can be induced by other chromophores or solvent molecules, for example. The intermolecular forces studied in this thesis are described in this section.

2.2.1 Solvent and environmental effects

Solvent and the environment can have profound effects on the spectral properties of chromophores. Solvent effects can be divided into general or specific solvent effects. If the solvent effects occur only in the excited state of the molecule, the changes are visible only in the emission spectrum. On the other hand, if the solvent interacts with the molecules in the ground state, the changes are visible before excitation, in the absorption spectrum for example. Solvent effects can also be weak in the ground state and the strength of interaction may increase after excitation. [1]

Solvent effects are a wide combination of several interactions with their local environment and can often be hard to explain. Some examples of the factors that can affect the emission spectrum and quantum yield of a compound include solvent polarity, rigidity of the local environment, internal charge transfer as well as proton transfer and excited state reactions. [10, 11]

The interactions between the solvent and the fluorophore alter the energy difference between the ground state and the excited electronic state. General solvent effects mainly include solvent properties such as the refractive index and dielectric constant of the solvent. Usually, the fluorophore has a larger dipole moment in the excited state than it does in the ground state. [1] In a polar solvent, this can result in reorientation or relaxation, which lowers the energy of the excited state. While the solvent polarity increases, the effect also increases with increasing polarity. This effect is most prominent with polar compounds. An increase in the solvent refractive index stabilizes the ground and excited states due to electron movements within the solvent molecules. This results in a lower energy of the excited state and the ground state. General solvent effects depend on the bulk properties of the solvent and do not alter the energy gap ΔE between the ground state and the excited state. [1]

Specific solvent effects include direct interactions with the solvent and they depend on the solvent and fluorophore properties. They are produced by only a few

molecules surrounding the fluorophore and can induce substantial changes in the emission spectra. Specific solvent effects most prominent to our case include hydrogen bonding, halogen bonding, and proton transfer reactions. Hydrogen bonding with solvent molecules, for example, lowers the energy of the excited electronic state resulting in a spectral shift to higher wavelengths. [1]

The fluorophore can also undergo intramolecular charge transfer (ICT). An ICT state can be a result of intramolecular proton transfer in the excited state. The initially excited state is usually called the locally excited state (LE). An internal charge transfer state occurs in emission spectra as emission at longer wavelengths. Changes between the LE and ICT state can manifest as a shoulder formation or a shift in the emission maximum. In low polarity solvents, the LE state is lower in energy and is the emitting species, whereas in high-polarity solvents, the ICT state is lower in energy. [1]

Solvent effects can be studied using different additives with predicted interactions with the fluorophore molecules in solution. Major spectral changes in very small percentages of additive indicate specific solvent effects rather than general effects. Specific solvent effects can also result in appearance of a new spectral component due to a chemical reaction. General solvent effects usually result in more gradual shifts in the emission spectra. In many cases, spectral changes due to interactions with solvent molecules can be a result of both general and specific solvent effects. [1]

2.2.2 Hydrogen bond

Hydrogen bonding (HB) has claimed its importance in many branches of science and continues to be an important subject of study. A hydrogen bond can be considered as a particular kind of dipole-dipole interaction. [12] It is an electrostatic interaction between a proton donor D-H and an electronegative proton acceptor A. [13] The proton donor does not necessarily need to be highly electronegative, but it is necessary to be at least slightly polar. [14] A general way to describe hydrogen bonding is using a water dimer. Interaction happens between two water molecules, where oxygen atom acts in both proton donor and proton acceptor moieties, described in Figure 2.3. [13] Hydrogen bonding can be linear, bent or bifurcated, for example.

Hydrogen bonding is considered to be a directional interaction, meaning that the bond formation is directional with the D-H bond. A hydrogen bond can be either intermolecular, occurring between two molecules or intramolecular, occurring within

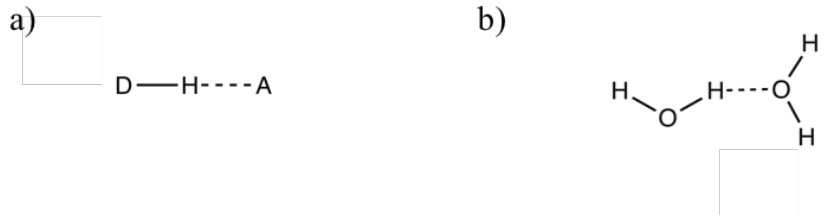

Figure 2.3 *a) Example of hydrogen bonding between the hydrogen bond donor (D–H) and an acceptor (A) b) water dimer with hydrogen bonding. [12, 13]*

the same molecule. Some sources claim hydrogen bonding to be a contact-like interaction, due to the necessity of orbital overlap. [13] Charge transfer in hydrogen bond occurs from the electron pair of a proton acceptor to an antibonding orbital of a proton donor $n_{\mathrm{Y}} \rightarrow \sigma^*{}_{\mathrm{DH}}$. The International Union of Pure and Applied Chemistry (IUPAC) loosely defines a hydrogen bond as "an attractive interaction between a group D-H and an atom or group of atom A in the same or different molecule(s), where there is evidence of bond formation". [15]

Hydrogen bond strength can range between 0.2 to 40 kJ mol^{-1}, landing it somewhere between the strength of Van der Waals interactions and covalent bonding. The bond strength varies widely depending on the molecules involved. [14] This wide variety of strengths indicates that the hydrogen bond is a combination of different interaction energies such as electrostatic, induction, electron delocalization, exchange repulsion, and dispersion interactions. [13] Depending on the exact proton donor-acceptor combination, all of these interactions affect with different weights. [14]

In a bifurcated situation, one molecule acts as a double proton donor, whereas another acts as a double proton acceptor. In these cases, hydrogen bonding is a nonlinear and relatively weak interaction. Since the hydrogen bond acceptor is usually an atom of high electron density, such as a lone pair, π-systems can also act as a proton acceptor in the formation of a hydrogen bond. [13]

Most systems containing a hydrogen bond are formed by two neutral molecules. Depending on the acidity and basicity of the interacting molecules, a hydrogen bond can also develop to be a proton-shared hydrogen bond. In this interaction, the length of the D-H bond is slightly increased, while the D-A distance decreases. The length of the interaction between the proton and the proton acceptor approaches the length of a covalent bond. In hydrogen-bonded ion pairs, the proton transfer occurs even further, slightly increasing the D-A and D-H bond lengths and decreasing the length of the A-H bond. The changes from a normal to a proton-shared to an ion-pair hydrogen bond depends on the degree of proton transfer and can be affected

by solvent and temperature effects. [13]

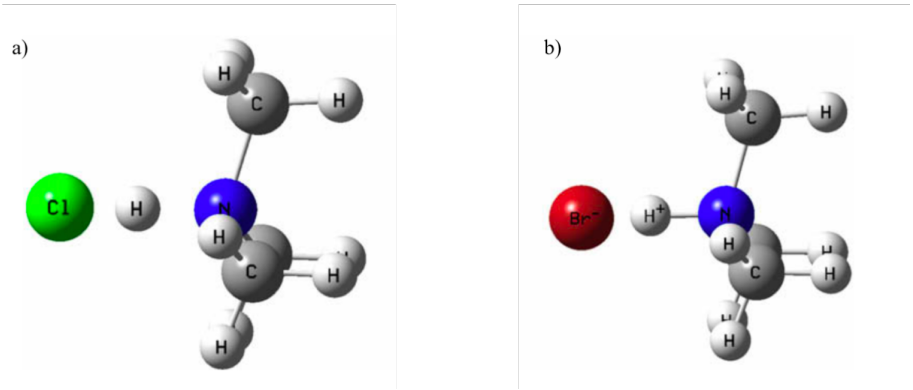

Figure 2.4 *An comparison of a) proton-shared hydrogen bond (HCl interaction with $N(CH_3)_3$) and b) ion-pair hydrogen bond (HBr interaction with $N(CH_3)_3$). [13]*

The special properties of hydrogen bonded systems, even after decades, continuously spark interest in further research. Hydrogen bonding between the chromophore and a solvent or a host matrix can have significant effects on a solution or film luminescence. Hydrogen bonding can reduce the mobility of the chromophores, lower the energy of the excited states and reduce aggregation. Hydrogen bonds are also important in biological systems, since they are responsible for the 3D structure of proteins, cellular recognition and the double helix structure of DNA. [12] In this thesis, the effect of hydrogen bonding on a compounds emission and lifetime is studied both in solution and the solid state.

2.2.3 Halogen bond

According to IUPAC, halogen bonding (XB) can be defined as an electrostatic interaction between an electrophilic region associated with a halogen atom in a molecular entity and a nucleophilic region in another, or the same, molecular entity.[16] Halogen bonding can be depicted as DX $\cdots$ A, where X is a halogen atom, D is considered as halogen bond donor and A as a halogen bond acceptor. The halogen bond acceptor donates electrons to the halogen bond, whereas the donor accepts electrons. Both halogen bond donor and acceptor tend to be electronegative moieties and quite often the bond acceptor is a Lewis base *i.e.* has a lone electron pair. [17]

Hydrogen is usually associated with having a positive partial charge, which makes it indisputable that it would interact with electronegative moieties. Halogens are usually associated with a negative charge, yet they participate in bond formation in a similar fashion as hydrogen in hydrogen bonding. Halogen bonding can be

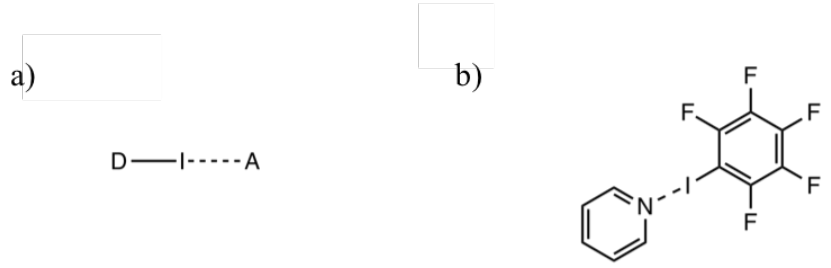

Figure 2.5 *a) Example of halogen bonding between the hydrogen bond donor (D–H) and acceptor (A) b) An example of halogen bonding between pyridine and commonly used halogen bond donor pentafluoroiodobenzene.*

explained using electrostatic potential, which has been found to be an effective tool for analyzing covalent interactions. [17] Electrostatic potential analysis reveals a region of positive electrostatic potential on the surface of the halogen atom as an elongation of the D–X covalent bond axis, also called the σ-hole. Because of this, halogen bonding tends to be highly directional with its electrostatic potential being aligned the D–X covalent bond axis, a typical bond angle being 180 °. [3]

The electrostatic potentials of halogen and hydrogen bond are described in Figure 2.6. The structures of the compounds 1a-c and 2 are presented above, and their electrostatic potentials range from -0.03 (red) to 0.03 (blue). The electrostatic potentials were calculated by Priimägi et al. using density functional theory. [18] The figure presents the same structure with either I, Br or H attached to the benzene ring. All compounds display positive electrostatic potential on the surface of I, Br or H. But from compound 1c, one can see, that the positive charge on the hydrogen atom is further distributed whereas the halogen bond is thought to be more directional, since the positive charge is more localized as an extension of the C-I covalent bond. [18]

It has been proven that the magnitude of the positive electrostatic potential depends on both the halogen (X) and the electron-withdrawing power of the rest of the molecule (D) [17]. The strength of the halogen bond interaction increases in the order of F $<$ Cl $<$ Br $<$ I, F being able to form halogen bonding only when attached to highly electron-withdrawing groups. [3] Tunability of the halogen bond strength makes it desirable in various applications. Halogen bonding can be used to modulate emission properties of systems in solution, solid-state and polymer martices. [19–23]

Halogen atoms have a double effect in inducing triplet-state emission; being electron acceptors and due to heavy atom effect. Heavy atom effect can be due to the heavy atom in the parent molecule (internal heavy atom effect) or the solvent (ex-

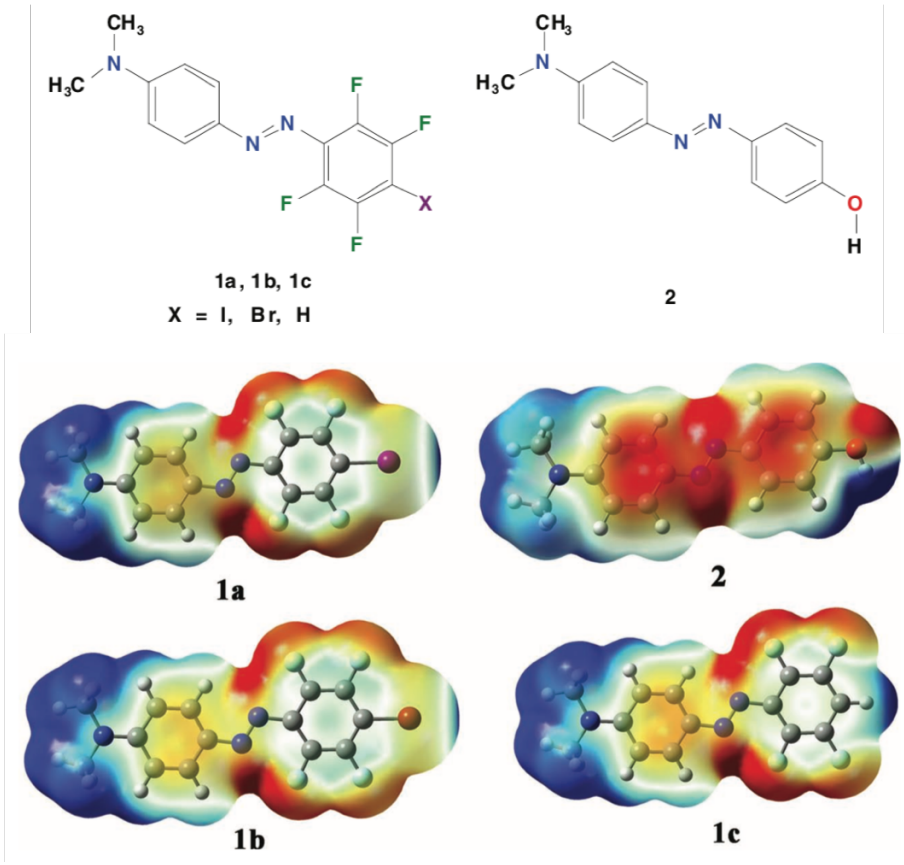

Figure 2.6 *Compounds 1a-c and 2 and their electrostatic potentials ranging from -0.03 (red) to 0.03 (blue). Figure describes the difference in electrostatic potential of the surface of halogen and hydrogen atoms. [18]*

ternal heavy atom effect), and it increases the probability of intersystem crossing by increasing the magnitude of spin-orbit coupling. [4, 22]

2.2.4 Ionic interactions

Electrostatic interactions between two atoms or molecules that involve an electron or proton transfer from one species to another are called ionic interactions. It is a type of chemical bonding that involves interaction between two oppositely charged ions. [24] Ionic interactions can be considered as a result of redox reactions or can be induced by acid-base reactions.

The difference between ionic bonding and covalent bonding is not always clear. In ionic bonding, the bond is formed by electrostatic interactions between two oppositely charged ions, whereas in covalent bonding the bond is formed by electron sharing between two atoms to attain more stable electron configurations. Covalent bonding is also considered to be more directional than ionic bonding. In the solid

state, atoms forming covalent bonds are packed according to the minimum energy principle where shared electron pairs repel each other. In ionic bonding, there are no repelling forces and ionic substances from tightly packed lattices in the solid state. [24]

Bonding can never be purely ionic, there is always some electron sharing occurring. This can be thought of as all ionic bonds having some covalent character. Whether a bond is classified as ionic or covalent depends on the difference of electronegativity between the bond forming atoms or ions. When the difference in the electronegativity is 1.7, the substance is usually associated with having 50 % of ionic character and 50 % of covalent character. Therefore, bonds with electronegativity differences over 1.7 can be taught of as ionic bonds.

When ionic bonds occur in the solid state, cohesive forces keep the lattice together and no single bond can be distinguished. In the case of a covalent bond, there is a more distinct bond between two atoms. Ionic compounds are also conductive in liquid and solid states and they can be utilized in electronic applications such as in the structures of OLEDs.

2.3 Polymers as optical materials

Polymers provide a considerable alternative to optical glasses. [25] They are becoming more and more common in the design of optical devices due to the wide range of properties that they provide and near infinite functionalization possibilities. [26] Polymers can be used as rigid matrices to reduce non-radiative relaxations and deactivation of excitation in luminescent systems. Incorporating luminescent materials in polymer matrices provides opportunities to improve the phosphorescence of these materials. [23] Polymer materials are desirable for optical applications also because of their low cost, simple solution processing, and tunable mechanical properties.

2.3.1 Polymer host-guest assemblies

Due to the wide variety of polymer structures, polymer-chromophore complexes with different functionalities can be designed. Various polymers have been used as hosts to incorporate chromophores (guests) into the polymer matrix. [27] The simplest way to introduce chromophores into polymer matrices is simply dissolving them in the same solution and preparing the film from that. In this case, the chromophores are randomly dispersed in the matrix. In a conventional host-guest assembly the polymer has virtually no interaction with the chromophore. Therefore,

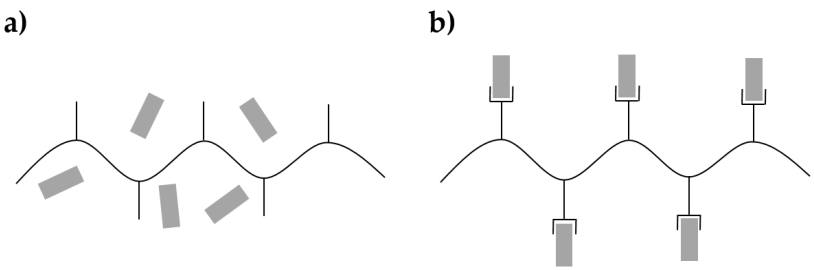

Figure 2.7 *a) Conventional polymer host-guest assembly with a high degree of chromophore mobility and b) decreased mobility in a polymer-chromophore complex.*

the chromophore has a high degree of mobility [28], which induces chromophore aggregation and phase separation, and thus reduces the optical quality of the system. [27]

Aggregation and phase separation limit the loading possibilities of the chromophores in conventional host-guest assemblies. Polymer-chromophore complexes use non-covalent interactions between the host polymer and guest chromophore molecules. [29] Polymer-chromophore complexes limit the guest-guest interactions and suppress the aggregation tendency of the chromophores. [27, 30] Furthermore, non-covalent bonding is a spontaneous event, which averts the need for multistep synthesis required when exploiting covalent bonding. [32] A reduction of the chromophore mobility is one of the most effective ways to reduce quenching and increase the phosphorescence quantum yield. [28] The conventional polymer host-guest assembly and polymer-chromophore complex with limited mobility are depicted in Figure 2.7.

The properties of polymer-chromophore complexes can be enhanced by functionalization of the polymer chain. Functional groups can provide formation of non-covalent bonds between the polymer and the chromophore. For example, the advantages of hydrogen bonding in polymer-chromophore matrices have been reported in different applications. [31] Modular functionalization of polymer chains by non-covalent bonding, such as hydrogen bonds, ionic interactions and metal coordination has been widely exploited. [32] In this thesis, the aggregation tendencies of the chromophore are reduced by exploiting hydrogen and halogen bonding in the formation of polymer-chromophore complexes. This is expected to increase the loading possibilities of the chromophore and therefore provide possibilities to enhance the systems luminescent properties. [27]

3. RESEARCH METHODS AND MATERIALS

This chapter describes the materials studied in this thesis, their characterization and emission modulation in solution and solid state. Moreover, this chapter includes methods used to prepare the samples and the instrumentation used for the characterization.

3.1 Materials

This section presents the materials studied in this thesis. This includes the luminescent materials that are used to exploit their light-emitting properties as well as the polymers that are used to rigidify the polymer-chromophore complexes and, possibly, enhance the phosphorescence of the chromophores. Various polymers are tested due to their possibilities to form non-covalent bonding with the chromophores.

3.1.1 Carbazole derivatives

Organic phosphorescent emitters are rare and usually based on toxic organometallic complexes. Many blue-emissive materials have been developed, but so far, they have not been optimal for commercial use due to short operational lifetimes when employed in OLEDs. [33] This thesis investigates the effect of intermolecular interactions in carbazole derivatives and their possibilities as blue-light emitters for applications in OLEDs.

Carbazoles are highly emitting materials commonly used in blue light emitting devices [34–36]. Here, benzophenone-carbazole and four of its derivatives are characterized with the aim of improving blue light emitting materials. The structure of benzophenone-carbazole (BpCz) is presented in Figure 3.1. To further enhance the interaction of the chromophore with the polymer matrix, benzophenone-carbazole was functionalized with pyridine and iodine substitutions. To analyze the effect of the added groups, the materials were prepared with one or two substitutions. The pyridine compounds could act as either HB or XB acceptors, whereas the iodine

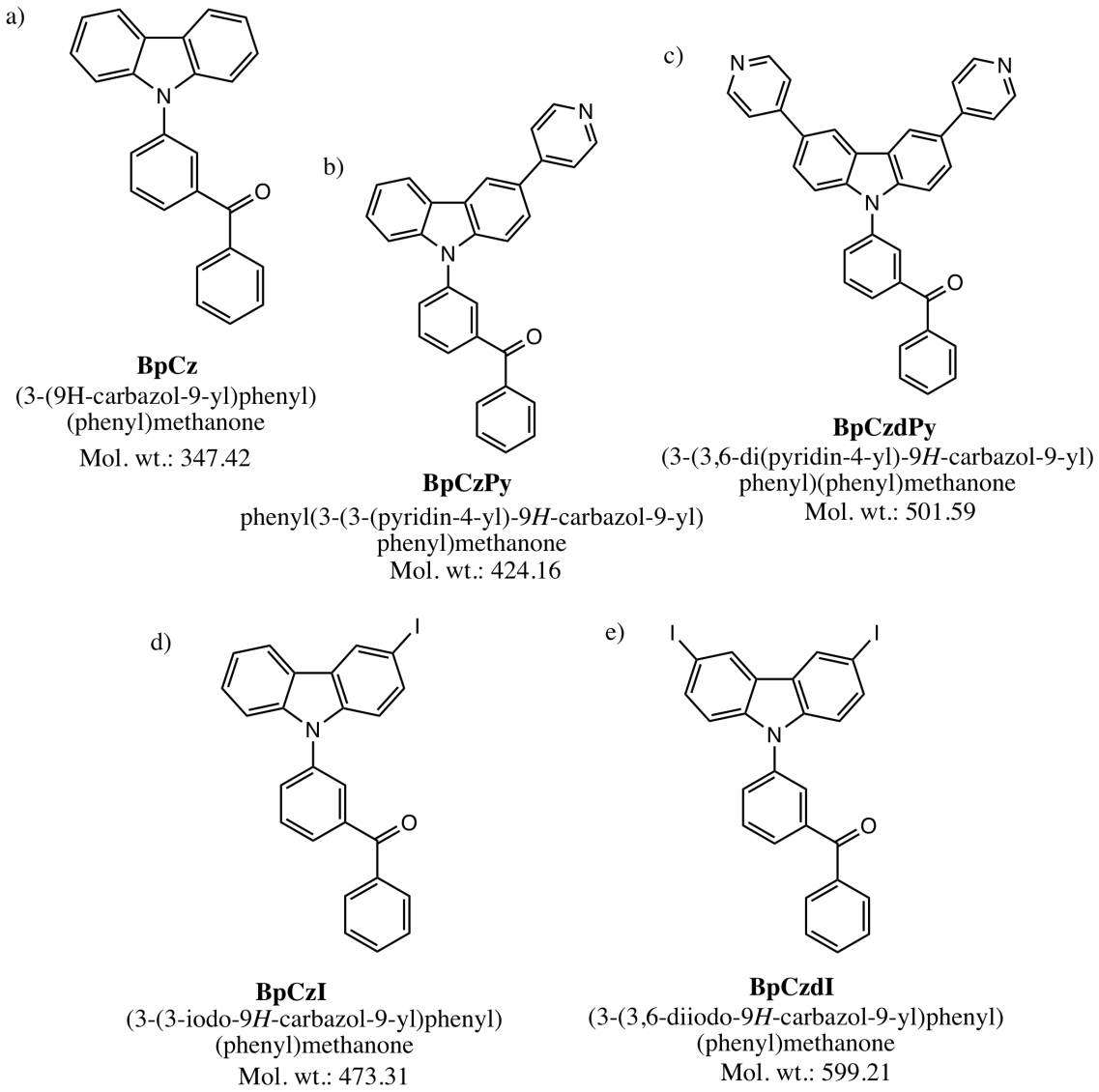

Figure 3.1 *The structures of a) BpCz and its derivatives b) BpCzPy, c) BpCzdPy, d) BpCzI and e) BpCzdI and their molar masses (g mol^{-1}).*

compounds could acts as XB donors. These structures are also presented in Figure 3.1. All the studied materials were synthesized in the Laboratory of Chemistry and Bioengineering of Tampere University of Technology by Mr. Jagadish Salunke. The synthesis of these materials is not included in this thesis.

Carbazole is a common fluorescent material due to its electron-rich core and easy tunability. [34] The carbonyl group in the benzophenone moiety as well as the halogen atoms in few of the derivatives make a significant contribution to the intersystem crossing and thus, are expected to induce phosphorescence. [2] In these emitters, the carbazole moiety acts as an electron donor and benzophenone acts as an electron acceptor. The addition of pyridyl groups should reduce the electron-donating

character of the carbazole core and therefore reinforce the emission. [33]

3.1.2 Polymers

Polymers are macromolecules that have high relative molecular masses, and they usually comprise of relatively simple repeating units. [37] They can be functionalized using different monomers and side groups in the polymer chain. For example, adding a hydroxyl group to a monomer significantly changes the properties of the polymer. The structures of all the polymers used in this thesis are presented in Figure 3.2. Polystyrene (PS) is one of the most widely used polymers in many industries. The structure of polystyrene is a carbon chain with benzene side group. Therefore, it is fairly unreactive and is used as a reference polymer in this thesis. Polystyrene is also one of the most transparent plastics. [38]

Other polymers used in this thesis were chosen for their functional side groups. Poly(vinyl phenol) (PVPh) was used to study the effect of hydrogen bonding in pyridine-containing compounds. The structure is similar to that of PS apart from the hydroxyl group attached to the 4-position of the benzene ring. This modification enables the formation of a hydrogen bond between the hydroxyl group and the pyridine nitrogen in the case of BpCzPy and BpCzdPy compounds. The effect of hydrogen bonding can now be observed by comparing both PS and PVPh samples to each other, and by the changes occurring with the addition of pyridine group from carbazole to BpCzPy and BpCzdPy.

The iodine compounds are capable of forming weak halogen bonds with their polymer matrices. To facilitate this, poly(4-vinyl pyridine) (P4VP) was used alongside with PS as a reference. Both PVPh and P4VP were chosen because of their structural similarities with the reference polymer (PS) to limit any differences in the properties of the films due to the structure of the polymer. P4VP has a pyridine group instead of a benzene ring, which enables it to form halogen bonding with the iodine compounds. The effect of halogen bonding can now be observed comparing carbazole, BpCzI and BpCzdI samples together and compare the differences in both the reference matrix and in the halogen bonding matrix.

Poly(styrenesulfonic acid) (PSS) is a conductive polymer that has benzenesulfonic acid group attached to a carbon chain. PSS is structurally similar to the other polymers used in these experiments, but it has an acid group that provides the possibility for ionic interactions. Ionic interactions can have significant effects on the luminescent properties of the films as described in section 2.2.3.

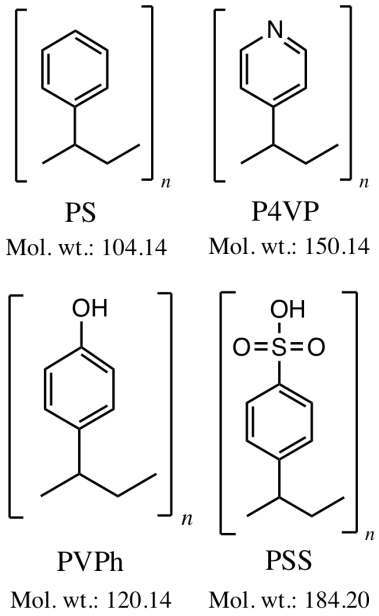

Figure 3.2 *The structures of repeating units of polystyrene (PS), poly(4-vinylpyridine), poly(vinyl phenol) and poly(styrenesulfonic acid) and their molar masses (g mol^{-1}). [38]*

3.2 Measurement methods

The compounds were first characterized in solution using dichloromethane (DCM) as a solvent. For the characterization, both steady-state and time-resolved methods were used, which are further described in the following sections.

Low temperatures and rigid media reduce the collisions and increase the possibility of observing phosphorescence. Under these conditions, the lifetime of the triplet state increases providing an opportunity to observe phosphorescence in the time-scale from milliseconds to minutes or more. [6] For this reason, the compounds were also embedded into polymer matrices to reduce the non-radiative relaxations in the system.

3.2.1 Steady-state spectroscopy

Steady-state spectroscopy methods are standard techniques in the characterization of new compounds. In this thesis, steady-state measurements include absorption spectroscopy to determine absorption of the samples and emission spectroscopy to characterize luminescent properties of the samples.

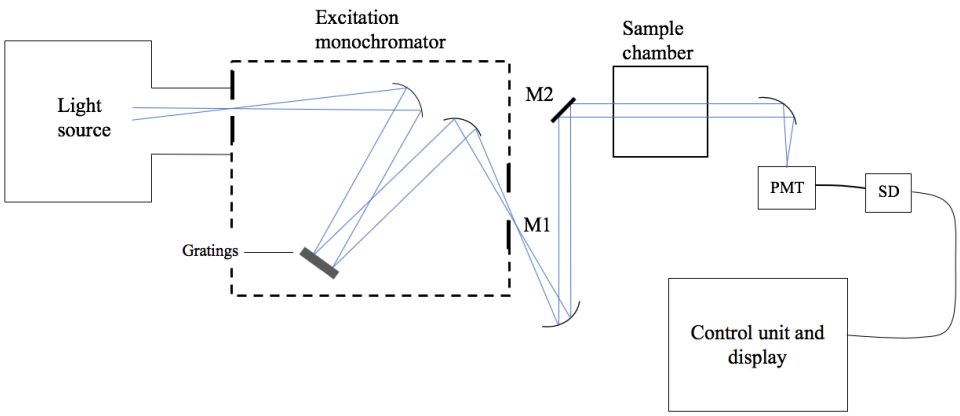

Figure 3.3 *A general scheme of one-channel spectrophotometer, where M1 and M2 are mirrors, PMT is a photomultiplier and SD is a synchronous detector. [39]*

Absorption Spectroscopy

Transmission spectroscopy is a relative measurement method that can provide information about the electronic subsystem of the matter. The absorption of the samples is determined using this method in this thesis. The instrumentation used to do this is generally called an absorption spectrophotometer. It consists of a light source, a sample chamber, and a detector. [39] The system can be one or two-channel instrument, of which the two-channel one is more precise and used in the absorption measurements of the liquid samples. [40] The one-channel scheme is presented in Figure 3.3. [39]

In principle, absorption spectroscopy measures the light intensity before entering the sample and the intensity of the light leaving the sample. The one-channel scheme has only the sample chamber, whereas the two-channel scheme consists of the sample chamber and a reference chamber. The remaining parts of the instrument are alike. [39] A general scheme of the two-channel instrument is presented in Figure 3.4. [39]

A light source consists of a lamp and a monochromator. The monochromator is used to select the wavelength entering the sample. [39] Diffraction gratings in the monochromator disperse polychromatic or white light into various wavelengths, which allows a certain wavelength to be selected. [1, 6, 39] A motorized monochromator enables automated scanning of wavelengths. To obtain a spectrum, measurements must be repeated in the desired wavelength range. From the monochromator, the light is focused into the reference chamber and sample chambers. [40] Part of the light is absorbed by the sample and the remaining light arrives at the detector, which consists of a photomultiplier tube (PMT) and synchronous detectors (SD).

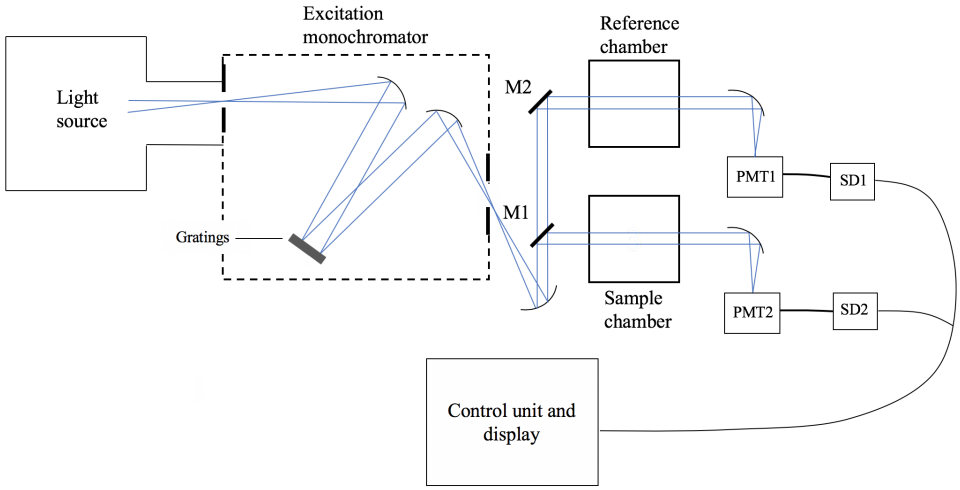

Figure 3.4 *A general scheme of two-channel spectrophotometer, where M1 and M2 are mirrors, PMT1 and PMT2 are photomultipliers and SD1 and SD2 are synchronous detectors. [39]*

The actual detected signal is voltage. The ratio of the voltages before and after the sample is equal to the ratio of the light intensities and can be used to calculate the transmission. [39] For the one-channel scheme

$$T(\lambda) = \frac{U_2(\lambda)}{U_1(\lambda)} \tag{3.1}$$

where T is the transmission, $U_1(\lambda)$ is the spectrum measured without the sample and $U_2(\lambda)$ is the spectrum measured with the sample. From Equation (3.1) the absorbance A can be calculated as

$$A(\lambda) = \log \frac{U_1(\lambda)}{U_2(\lambda)} \tag{3.2}$$

In the two-channel scheme, the light from the reference chamber is used as a "light before the sample" since the reference chamber does not contain the absorbing sample of interest. The two-channel scheme also enables one to measure the absorption of a molecule in a solvent, by inserting a similar cuvette with the same solvent into the reference chamber and therefore, discarding the absorption of the solvent from the calculation. Thermal fluctuations that might affect the spectrum are also discarded in the two-channel scheme since the reference and the sample spectra are recorded simultaneously. [39]

A recorded spectrum without a sample is called a baseline and is used to eliminate

distortions from the sample spectrum due to the instrument. It is measured before starting sample measurements to correct the differences between the reference and sample chambers. If $R(\lambda)$ is the ratio of the voltages from the sample and reference chambers measured without the sample and $S(\lambda)$ is the ratio of the voltages from the sample and reference chambers measured with the sample, then the transmission can be calculated for the two-channel scheme [39]

$$T(\lambda) = \frac{S(\lambda)}{R(\lambda)} \tag{3.3}$$

Generally, one can decide the accumulation time (dwell time) of the measurement at each wavelength. This can be used to improve measurement quality since longer accumulation time provides greater signal-to-noise ratio. [39]

Emission spectroscopy

Like absorption spectroscopy, emission spectroscopy is a routine method in the characterization of new compounds. A compound is excited at a certain wavelength and a fluorescence spectrum is recorded. The fluorescence spectrum is the energy spectrum of the photons emitted during the relaxation of the excited state. It provides information about the electronic states of the matter and is a sensitive method that can be used to study even a single molecule. [39]

Emission is measured by keeping the excitation wavelength constant and scanning the detection wavelength to measure a spectrum. The selection of excitation wavelength depends on the subject under investigation and its absorption spectrum. Detection wavelengths can vary but should be selected so that the whole emission spectrum can be recorded.

Most instruments can record both emission and excitation spectra. Excitation spectrum describes the dependence of excitation wavelength on emission intensity and depicts the relative amount of excitation throughout the spectrum. It is measured by keeping the emission wavelength constant, generally at the emission maximum, while scanning the excitation wavelength. Usually, the excitation spectrum closely resembles the absorption spectrum of the sample, but might not be identical, since the excitation spectrum only displays the absorption bands that contribute to the fluorescence of the molecule. [41] The light source is usually wavelength-dependent, and the intensity of the excitation source is not constant throughout the spectrum. To obtain accurate excitation spectra, a correction spectrum must be used. [1]

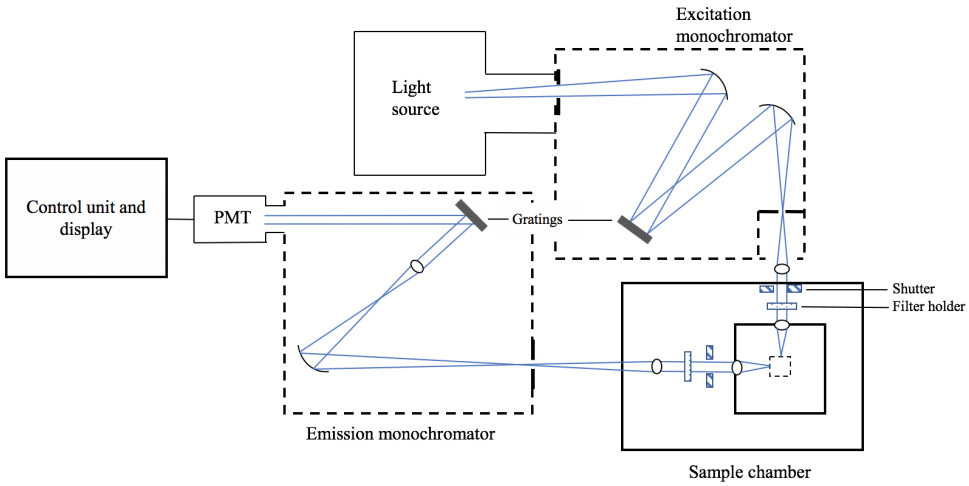

Figure 3.5 *A general scheme of emission spectrofluorometer. [1]*

Instrumentation used for fluorescence measurements is usually called a fluorimeter or spectrofluorometer. The main parts of the instrument consist of the excitation source, the sample chamber, and a detector. [39] This equipment can vary from instrument to instrument. A general scheme of a fluorimeter is presented in Figure 3.5, [1] in which the emission is collected in a right angle. The excitation source consists of a light source and a monochromator. Generally the light source is a xenon arc lamp, because it has high intensity from 250 nm to the near infrared. [6] An excited sample emits light in all directions and the instrument should be able to collect as much as possible of the emission. [39]

Monochromators are used in fluorimeters as in the absorption spectrophotometers. In addition to monochromators, optical filters can be used, which can limit the wavelengths that are detected. They can be used to confine errors due to scattered or stray light or to exclude the second order diffraction from the monochromators. Shutters are used to eliminate the excitation light or shut the light to the emission monochromator. [1]

The detection part of the instrument collects the emitted light. This is done using an optical lens. The emission monochromator and a photomultiplier tube are used to detect the collected light. Monochromator slits determine the bandwidth of the light entering the PMT, so only the photons emitted in a concise bandwidth $\Delta\lambda_{em}$ are detected. Larger monochromator slits provide larger signal intensity, but also increase the bandwidth, which lowers the resolution. Total emission of the sample can be determined by integration of the emission spectrum. [1]

In absorption spectroscopy, the light intensity is measured relative to a reference,

thus, the wavelength-dependencies of the instruments are not a factor. [1] In emission spectroscopy, the correct emission spectrum of the sample is obtained after removing the wavelength-dependencies of the instrument by applying a correction spectrum supplied by the manufacturer. [39]

3.2.2 Time-resolved spectroscopy

Time correlated single photon counting is a time-resolved emission measurement technique, which is extremely sensitive and in extreme cases allows one to study even a single molecule. Fluorescence intensity is proportional to the population of the excited state. Emission lifetime is defined as the time τ in which the population of the excited state is reduced to 1/e of its initial value. Detection of time-resolved emission enables to determine the sample emission lifetime. TCSPC is one of the most accurate measurement techniques to study emission lifetimes in the nano- and subnanosecond time domains. [39]

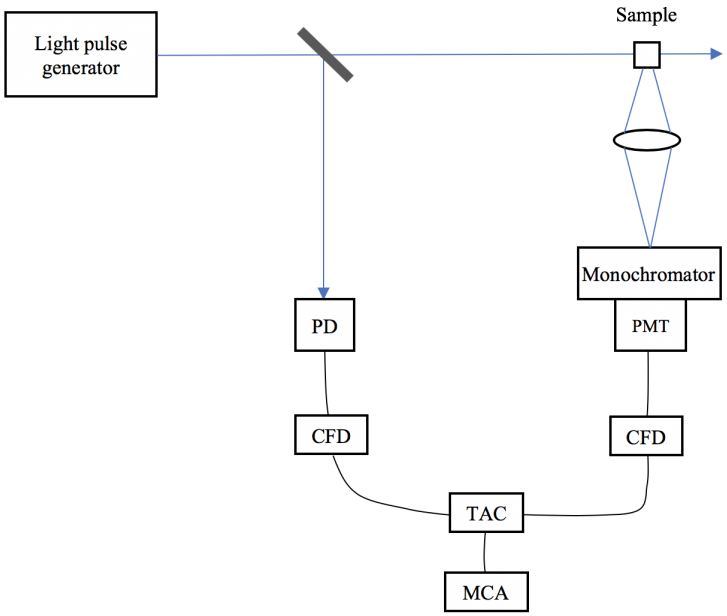

Figure 3.6 *A general scheme of time correlated single photon counting instrument, where PD is a photodiode, CFD is a constant fraction discriminator, TAC is a time-to-amplitude converter and MCA is a multichannel analyzer. [39]*

A general scheme of TCSPC instrumentation is presented in Figure 3.6. A pulsed excitation source is used as a source of excitation light. A short light pulse is split into two routes by a glass or quartz plate. The first route goes straight to the detection system and acts as a start pulse. The other route excites the sample and the emission is collected at the selected wavelength by the detection system. The

first photon arriving at the detector acts as a stop signal and the time between these two signals is used to calculate the emission lifetime. [39]

The excitation source is typically a pulsed LED or a sub-nanosecond solid state laser, which has a relatively narrow pulse width and is suitable for measurements in the nanosecond time domain. [1] A small part of the excitation light is directed to a pulse triggering photodiode (PD). The light which passes through the sample is collected by a lens, and directed to a monochromator. A small range of the emission is collected by the detector, usually around the emission maximum. Each photon hitting the photomultiplier generates an electric pulse on the photomultiplier output. The electric pulses from the PD and PMT are directed to a constant fraction discriminators (CFD), which determine the timing of the two different pulses. From the CFD, the pulses are directed to the time-to-amplitude converter (TAC), which is a voltage generator that ramps the voltage linearly with time in a nanosecond timescale. [1] The pulse from the PD starts the generator and the photon from the emission stops it. The output voltage is directly determined by the time difference between the two pulses. A multichannel analyzer (MCA) analyzes the output voltage and collects an emission time profile. [39]

For the emission decay to be measured, the sample must be excited multiple times. For most of the pulses, there are no photons detected. Typically, the detection rate is 1 photon per 100 excitation pulses. [1] The repetition rate of the excitation pulse must be adjusted depending on the nature of the sample. For samples with long lifetimes, and therefore long relaxation times of the excited state, a high repetition rate might be unacceptable. If the sample is not fully relaxed, the arriving pulse will excite an already excited state. [39]

The result of a TCSPC measurement is an emission decay. Measuring emission decay at various wavelengths provides a time-resolved emission spectrum. Usually, three curves are presented in the results. These are instrument response function (IRF), emission decay and the fit curve. An example of an TCSPC result is presented in Figure 3.7. IRF represents the response of the instrument to an empty sample chamber, and it is characteristic to the detector and timing instruments. [1] The fit curve is a convolution integral of the measured intensity decay and the IRF. If the IRF is $r(t)$ and the sample response is $s(t)$, then the experimentally measured signal is given by

$$s(t) = \int_{-\infty}^{t} r(\tau) f(t-\tau) d\tau \tag{3.4}$$

This can be used to accurately fit the measured data taking into account the response

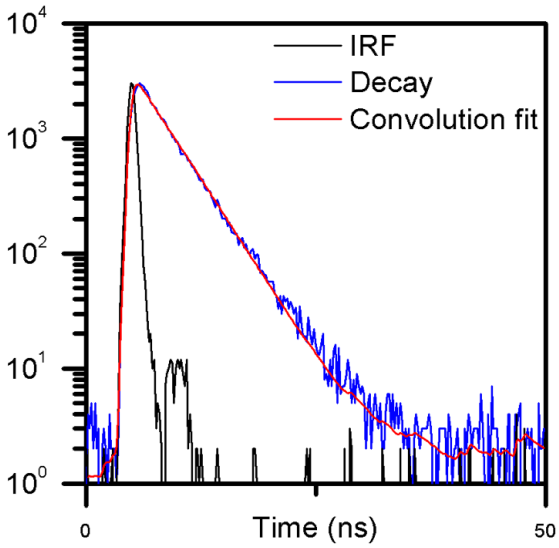

Figure 3.7 *An example of time-correlated single photon counting data and fitting.*

of the instrument. In this thesis, TCSPC technique was used to characterize samples in both liquid and solid state.

3.2.3 Topographical studies

Wyko Surface Profiler was used to determine the thickness of the polymer-chromophore film on quartz substrates. The instrument uses phase-shifting interferometry, which is a non-invasive technique. A filtered white light is passed through an interferometer objective to a beamsplitter, from which half of the light travels to the surface of the sample and half to the reference. The beams from the sample and the reference are reflected back and recombine to form interference fringes. A piezoelectric transducer moves the reference surface causing a phase shift between the two beams resulting in an interference pattern. This collected phase data can be used to calculate the surface height of the sample [42]

$$h(x,y) = \frac{\lambda}{4\pi}\phi(x,y) \tag{3.5}$$

where $h(x,y)$ is the height and $\phi(x,y)$ is the phase shift. The surface roughness of the samples was studied using digital holographic microscope (DHM). DHM provides quantitative phase contrast imaging that is suitable for high resolution imaging of reflective surfaces. DHM uses typically a Nd:YAG laser as a source of coherent light. The light is split into object illumination and reference wave. The light used for sample illumination is coupled into the optical path of the microscope's condenser

by a beam splitter cube. The light reflected from the sample is passed through a second beam splitter with a slight tilt to create two "off-axis" holograms recorded by a digital image sensor (camera). From the camera, the holograms are transmitted to an interface which produces the image. [43]

From DHM measurements, the roughness parameters S_a, S_q, S_{ku} and S_{sk} were determined. S_a represents the roughness average of the surface and is the mean of the absolute values of the surface departures from the mean plane. S_q is the root mean square of the surface roughness and it represents the standard deviation of the surface heights. S_{ku} is the kurtosis of the surface and gives information on the spikiness of the surface. Lastly, S_{sk} is the skewness of the surface and measures the asymmetry of the plane. [42] For an optimal surface, these values are expected to be small with only slight variation.

3.3 Experimental

The experimental work of this thesis was conducted in the Laboratory of Chemistry and Bioengineering in Tampere University of Technology. It entails basic spectroscopic characterization of the carbazole derivatives as well as the preparation of polymer solutions and polymer-carbazole films. The experimental section also includes several titration series to further study the properties of the carbazole derivatives in solution.

3.3.1 Solutions

Characterization of carbazole derivatives was done by absorption and emission spectroscopy. To avoid spectral distortions due to high concentration, 10 μM solutions were prepared. Several solvents were tested for good solubility of the compounds. All of the compounds were easily soluble in chlorinated solvents and the solutions were prepared out of DCM. This yielded desired absorbances around 0.2-0.4 at the excitation wavelength for the emission measurements. Absorption spectra were recorded from 240 nm to 500 nm using quartz absorption cuvettes since the samples were expected to have absorption in the UV range of the spectrum. Absorption spectra of the solutions were recorded using Shimadzu UV-3600 UV-Vis-NIR spectrophotometer.

The excitation wavelength for the emission measurements was selected so, that all the compounds had a relatively good absorbance at that wavelength, close to absorbance maximum. Also, a factor in the wavelength selection was the laser choices

for the lifetime measurements. It was desirable to determine both emission spectra and lifetimes using the same excitation wavelength. For this reason, excitation was chosen at 340 nm. To record the whole emission spectra, monitoring wavelengths were chosen from 350 to 700 nm. All excitation spectra were recorded from 240 nm to 500 nm and monitored at the emission maximum. For all measurements the excitation and emission monochromator slits were set to 1 nm width and quartz fluorescence cuvettes were used. The excitation and emission spectra were recorded using Edinburgh Instruments FLS1000 spectrometer.

The lifetimes of the samples were determined using time correlated single photon counting -technique. The measurements were performed using PicoQuant PicoHarp 300 TCSPC system. The samples were excited using both 340 nm and 375 nm excitation.

Emission quantum yield measurements

A concentration series was prepared to determine emission quantum yields for the compounds. 9,10-Diphenylanthracene (DPA) was chosen for reference compound and solutions with roughly 0.03, 0.05, 0.07 and 0.1 absorbances were prepared from cyclohexane. For the reference compound, the emission quantum yield was presumed to be unity. All sample solutions (BpCz, BpCzPy, BpCzdPy, BpCzI, and BpCzdI) were prepared in DCM with similar concentration series. The absorbance and emission of these solutions were measured as mentioned previously.

Total emission intensities were determined by integrating the emission spectra. Plotting the emission intensities as a function of absorbance enabled to determine the emission quantum yields using Equation (2.4). An example of the linear fitting in the determination of the quantum yields is presented in the results section.

Titration series

Several titration series were prepared in order to investigate non-covalent bonding in solution and its effects on emission modulation. Titration series were prepared starting with 10 μM solutions of the samples in DCM. 5 ml of the solutions were titrated with pentafluoroiodobenzene, phenol and benzenesulfonic acid. In between each addition, the emission and absorption spectra, as well as excited-state lifetimes of the solutions were recorded. The structures of the additives are presented in Figure 3.8.

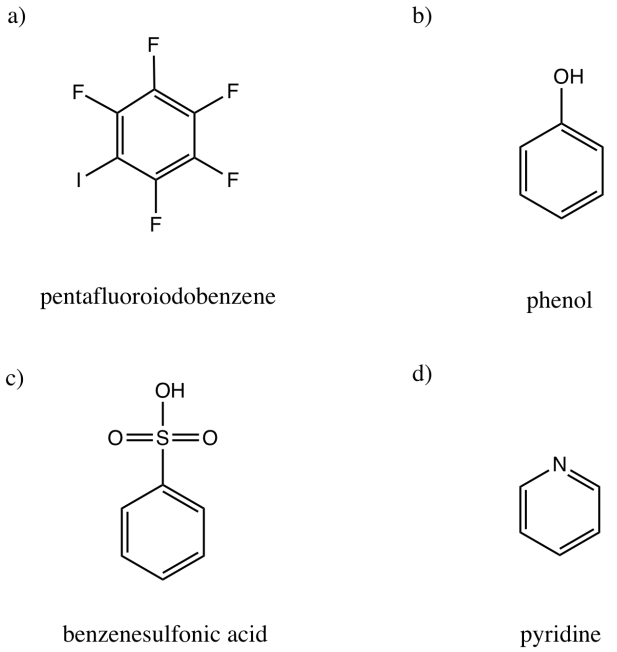

Figure 3.8 *The structures of a) pentafluoroiodobenzene b) phenol c) benzenesulfonic acid and d) pyridine used in the titration series.*

Pentafluoroiodobenzene (PFIB) is a commonly used XB donor that was used in this thesis to form halogen bonding to the pyridyl group of the BpCzPy and BpCzdPy. The carbazole core enhances the Lewis basic character of the pyridyl group and therefore strengthens the halogen bond. [19] Phenol is a weak acid that can be used as an HB donor molecule, while the pyridine compounds act as acceptor molecules. Benzenesulfonic acid (BSA), however, is a strong acid that could possibly interact with the pyridine compounds forming an ion-pair hydrogen bond or protonation of the pyridyl group. One titration series was also performed using BpCzI and BpCzdI as XB donors. In these compounds, the iodine atom is not very highly polarized, but could still form weak halogen bonding. The series was prepared using pyridine as the XB acceptor.

3.3.2 Films

Polymer-chromophore films were prepared from various polymers mentioned in section 3.1. Since some of the polymers are highly polar due to their side groups, DCM was not a suitable solvent for all of the films. A compromise was made, and BpCzdPy was ruled out from the film studies due to its many solubility issues. PVPh and PS have very different properties, and a common solvent for both of these polymers and all the samples was not found.

Polar polymers (PVPh, P4VP, and PSS) were dissolved in dimethylformamide (DMF), whereas the nonpolar polymer (PS) was dissolved in tetrahydrofuran (THF). BpCz, BpCzPy, and BpCzI were all soluble in these solvents, even in high concentrations. BpCzdPy was not soluble at all, and BpCzdI only in small concentrations.

A polymer stock solution was prepared in 6 mol-% concentration in comparison to the solvent. This value was kept constant throughout the experiments. A mole percent can be defined as the percentage of the total moles in the solution. In polymer solutions, the amount of substance is determined based on the molar mass of the monomer unit. A few milligrams of the sample was weighted and polymer stock solution added to that according to the desired concentration.

The films were prepared onto quartz substrates. The substrates were cleaned using a sonicator. At first, the samples were sonicated with chloroform for 10 min, then with isopropanol and lastly with Milli-Q water for 10 minutes. The substrates were dried with N_2. After this, the polymer-chromophore solutions were spin coated onto the quartz substrates. The program used for the spin coater is presented in Table 3.1.

Table 3.1 *The spin coating program used in the preparation of polymer-chromophore films.*

Speed	Acceleration	Time	Added volume
3000 rpm	3000 rpm/s	30 s	80–200 μ l

All the films were characterized using absorption and emission spectroscopy as well as TCSPC. The film surface was studied using optical profilometer to determine the film thickness and digital holographic microscope to study the surface roughness of the samples.

4. RESULTS AND DISCUSSION

This chapter presents the experimental data obtained during the implementation of this thesis. The compounds presented in the materials section were first characterized in solution. Interactions due to non-covalent bonding in solution were studied with several titration series, which are all described here. The compounds are also characterized in the solid-state and the effects of non-covalent bonding are studied in polymer matrices.

4.1 Characterization of carbazole derivatives in solution

This section presents all the results from the experiments done in solutions. These include characterization using basic spectroscopic methods, lifetime measurements, determination of emission quantum yields and the results from the titration series.

4.1.1 Carbazole derivatives in solutions

The characterization of the aforementioned compounds was performed first using absorption spectroscopy. The molar absorption coefficients for the samples were determined by preparing solutions with precise concentration and measuring the absorbances of the samples. The molar absorption coefficients of BpCz, BpCzPy, BpCzdPy, BpCzI, and BpCzdI are presented as a function of the wavelength in Figure 4.1.

All the carbazole derivatives absorb light in the UV-region of the spectrum. The absorbances of the samples are very similar in a way that three absorption bands occur in all of the samples. In both pyridine and iodine cases, the addition of a new group to the carbazole core increases the absorbance of the sample. The absorption band around 300 nm for BpCzPy and BpCzdPy can be localized on the pyridylcarbazole donor based on time-dependent density functional theory calculations (TDDFT) carried out by Rajamalli et al. [33] The band at 340 nm can be assigned to the intramolecular charge transfer from the carbazole moiety to the benzophenone. [33]

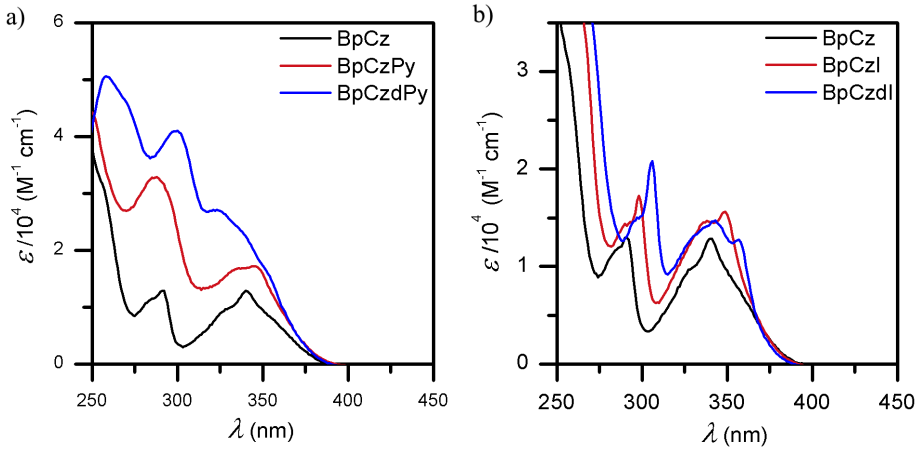

Figure 4.1 *The molar absorption coefficients ϵ of the carbazole derivatives as a function of the wavelength λ.*

The addition of an iodine to the carbazole core increases the absorbance while shifting it to the higher wavelengths. Going from BpCz to BpCzI and BpCzdI, the absorbance band around 300 nm becomes more distinct and a new absorbance shoulder develops at 340 nm. In the case of BpCzdI, this shoulder increases even more and changes the shape of the spectrum.

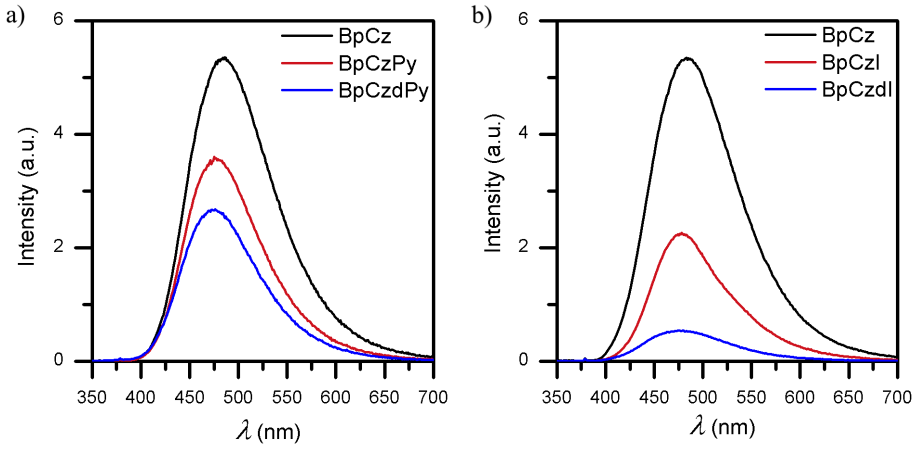

Figure 4.2 *The emission intensities (a.u.) of the carbazole derivatives as a function of wavelength λ. The samples were excited at 340 nm.*

The emission spectra of the samples are presented in Figure 4.2. All the compounds show broad emission spectra in DCM. BpCz has an emission maximum λ_{max} at 487 nm, whereas BpCzPy has an emission maximum at 481 nm and BpCzdPy at 473 nm. The addition of pyridyl group slightly lowers the emission wavelengths and decreases the emission intensity due to the electron-withdrawing nature of the pyridyl ring.

Similar effects can be observed in the case of the iodine compounds. BpCzI has an emission maximum λ_{max} at 478 nm and the BpCzdI at 475 nm. Heavy atoms in a molecule promote intersystem crossing, thus increasing the phosphorescence quantum yield. This can be seen as a decrease in the emission since the phosphorescence is readily quenched by atmospheric oxygen. [4]

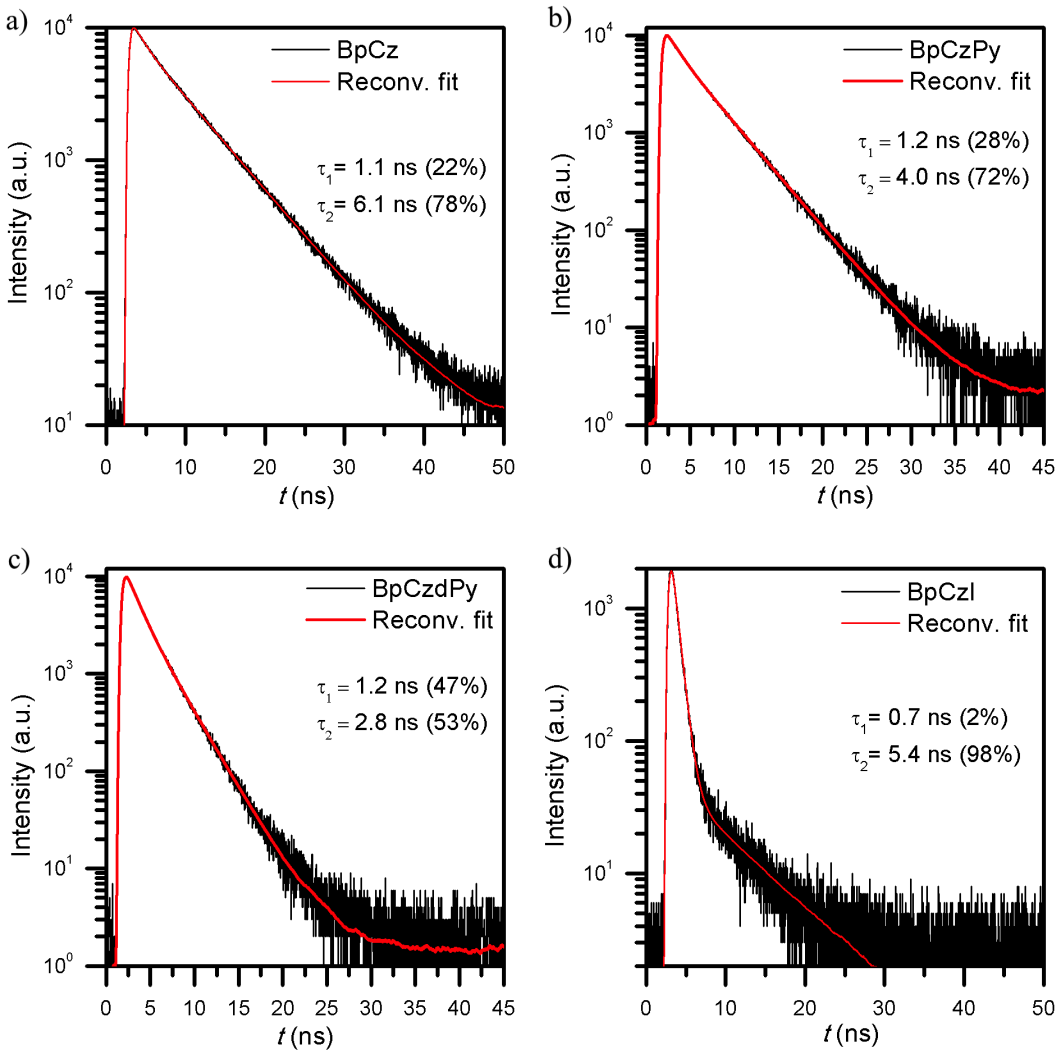

Figure 4.3 *The results of emission lifetime measurements of a) BpCz b) BpCzPy c) BpCzdPy and d) BpCzI in DCM solutions using excitation at 340 nm.*

The emission lifetimes of the samples were determined using TCSPC. All the lifetimes of the compounds in solution were determined using biexponential convolution integral to fitting of the data. BpCz has an emission lifetime of 6.1 ns (78 %) and 1.1 ns (22 %). BpCzPy has lifetimes of 4.0 ns (72 %) and 1.2 ns (28 %), BpCzdPy 2.8 ns (53 %) and (47 %), and lastly, BpCzI 5.4 ns (98 %) and 0.7 ns (2 %). The emission lifetime of BpCzdI compound was not determined due to its very low emission intensity.

Determination of emission quantum yield

The emission quantum yields of the compounds were determined in DCM using a concentration series and linear fitting. Exact absorbances and integrated total emission intensities were used in the calculation of the slope, the values of which are listed in Table 4.1. The table also lists the refractive indices of the used solvents and the calculated emission quantum yields. An example of the linear fitting of the data is presented in Figure 4.4.

Table 4.1 *The value of the slope of the linear fit of emission intensity against absorbance, solvent refractive indices, and emission quantum yields of the carbazole derivatives.*

Sample	Slope	Refractive index (solvent)	Quantum yield
9,10-Diphenylanthracene	13.53	1.4242	100.0 %
BpCz	3.53	1.4235	26.1 %
BpCzPy	2.57	1.4235	19.0 %
BpCzdPy	2.08	1.4235	15.3 %
BpCzI	1.66	1.4235	12.0 %
BpCzdI	0.63	1.4235	4.55 %

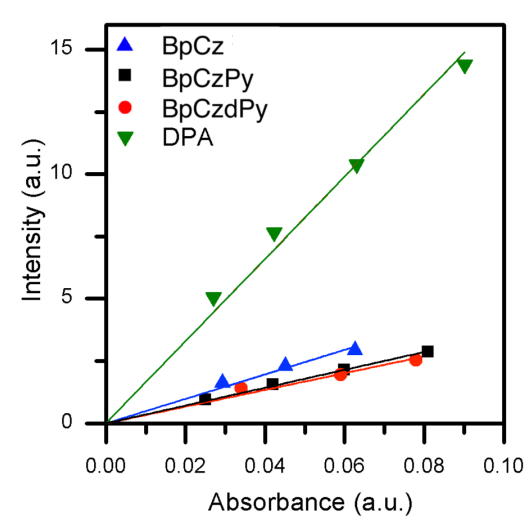

Figure 4.4 *An example of the linear fitting used in determination of the emission quantum yields, where intensity I of the emission is plotted against absorbance* (A) *of the sample at the excitation wavelength 340 nm.*

By using equation (2.4) the emission quantum yield of BpCz was determined as 0.26, BpCzPy 0.19, BpCzdPy 0.15, BpCzI 0.12 and BpCzdI 0.05. Room temperature phosphorescence from organic compounds is rare and nearly non-existent in solution. Therefore, the observed quantum yield can be assumed to be fluorescence quantum yield. The quantum yields of the samples decrease with the addition of

pyridyl or iodine groups to the carbazole core. This is assigned to the increase in phosphorescence quantum yield, which is not observed due to oxygen quenching. [4]

4.1.2 Pentafluoroiodobenzene titration series

The titration series was performed to study non-covalent bonding in solution. The structure of PFIB is presented in the experimental section in Figure 3.8 and the absorption spectrum in Figure 4.5. The results of the absorbance measurements with the addition of PFIB are presented in Figure 4.6. In BpCz spectra, the changes occur in the region of PFIB absorbance. Since PFIB has no interaction with BpCz, it should not affect the absorbance bands out of PFIB absorbance region. Therefore, the absorbance previously assigned to intramolecular charge transfer from carbazole to benzophenone remains the same.

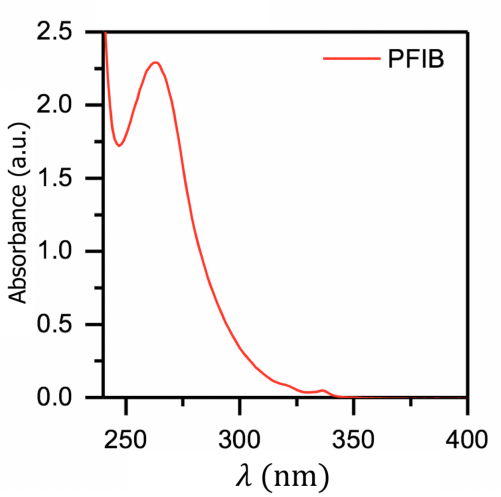

Figure 4.5 *The absorbance* (A) *of PFIB as a function of wavelength* (λ).

The absorbance of BpCzPy and BpCzdPy experience similar changes in their spectra. The intensity of the spectra increases with the addition of PFIB and both spectra have an isosbestic point around 340 nm. In both BpCzPy and BpCzdPy spectra, a new absorbance band appears around 380 nm, which can be assigned to intramolecular charge transfer to the pyridine moieties after halogen bonding.

The results of the emission measurements of the titrated solutions are presented in Figure 4.7. The addition of PFIB to BpCz solution resulted in no changes in the small concentrations. After a significant addition of PFIB, the emission intensity of BpCz decreased slightly. BpCz compound has no halogen-bond acceptor moiety, and thus, should have no interactions with PFIB. The increasing PFIB absorbance reduces the BpCz absorbance and therefore the addition of PFIB shows up as a

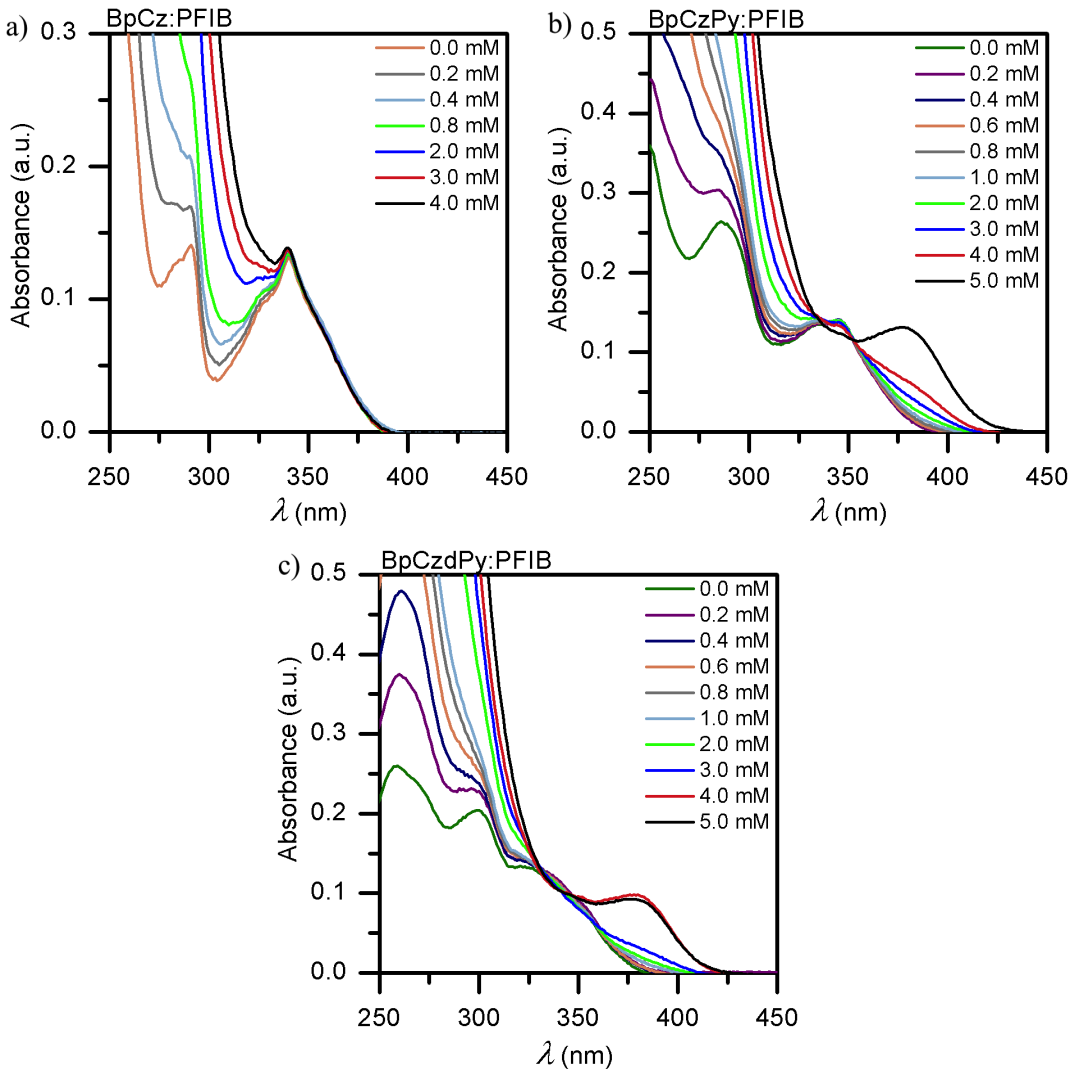

Figure 4.6 *Absorbances of the titration series with pentafluoroiodobenzene.*

decrease in the emission intensity of the solution. The emission maximum remained at roughly the same position and no spectral shifts occurred.

In the case of BpCzPy and BpCzdPy samples, the emission intensity increases with the addition of PFIB. The differences in the increase can be seen from Figure 4.7d. This figure presents the relative integrated emission intensity change as a function of the added PFIB concentration. Each measurement point represents the change in emission intensity that occurs in respect to the zero PFIB concentration point. The emission intensity of BpCzdPy increases more significantly than in the case of BpCzPy, though both experience an increase that behaves in the same manner. In the case of BpCzdPy, the emission maximum also experiences a blue-shift of 25 nm.

The increase in emission intensity seems to be linear having two different slopes. At

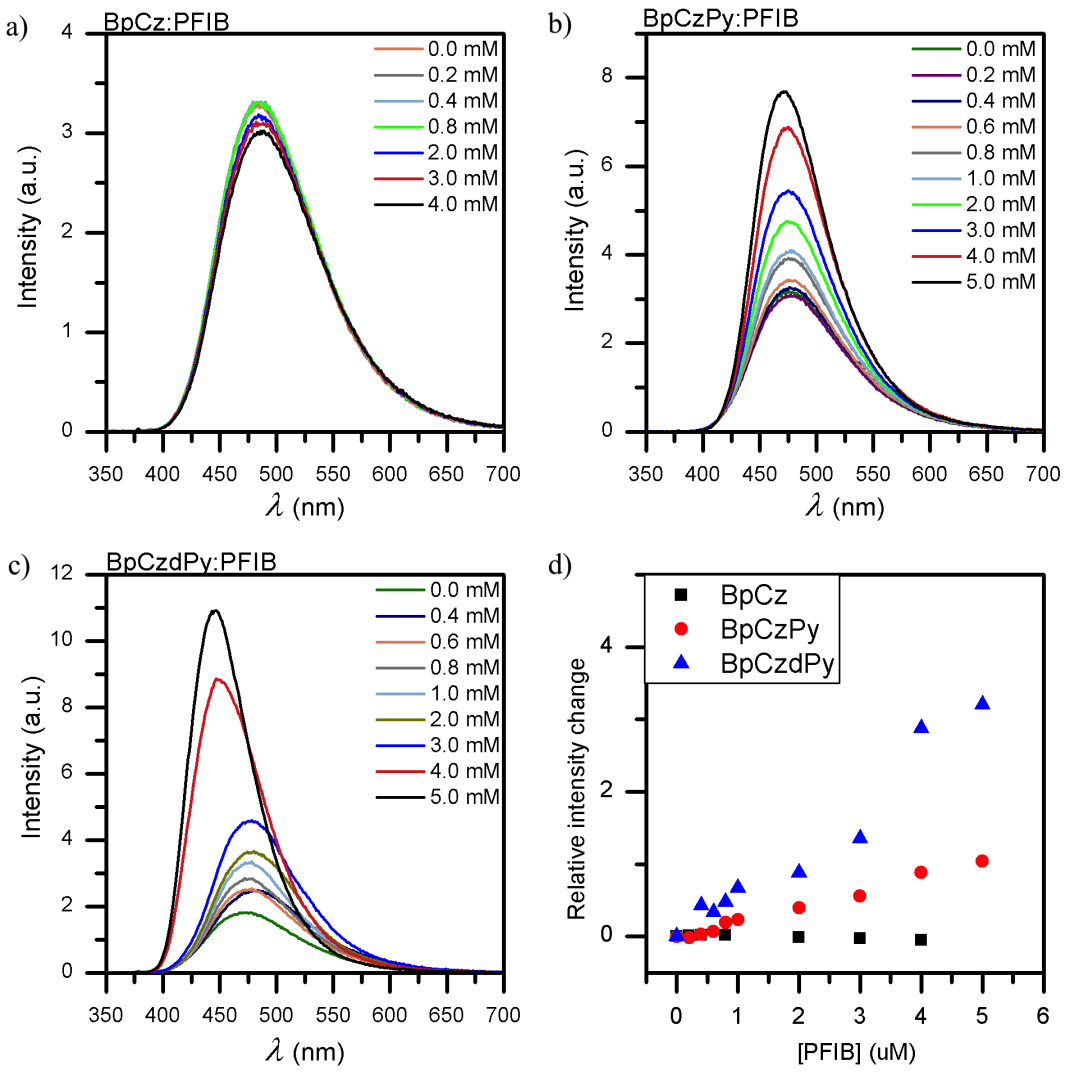

Figure 4.7 *Emission intensities of the titration series with pentafluoroiodobenzene. Figure d) presents the integrated relative intensity change.*

first, the intensity increases very rapidly until the change slows down, still upholding its linear form. BpCzPy is able to form halogen bonding with the iodine in PFIB. Halogen bonding in these systems induces intramolecular charge transfer, which modulates the emission properties of the system. This has been previously shown in literature. [19] In the case of BpCzdPy, there are two halogen bond-acceptor moieties, it having two pyridyl groups. Therefore, the increase is roughly twice as high.

Lifetimes of the samples were studied during this titration series. Changes in the quantum yields and the longest component of the lifetime are presented in Figure 4.8. Both components of the lifetime and their percentages are presented in the Appendix A. The lifetime of BpCz increases approximately 0.5 ns, which approaches

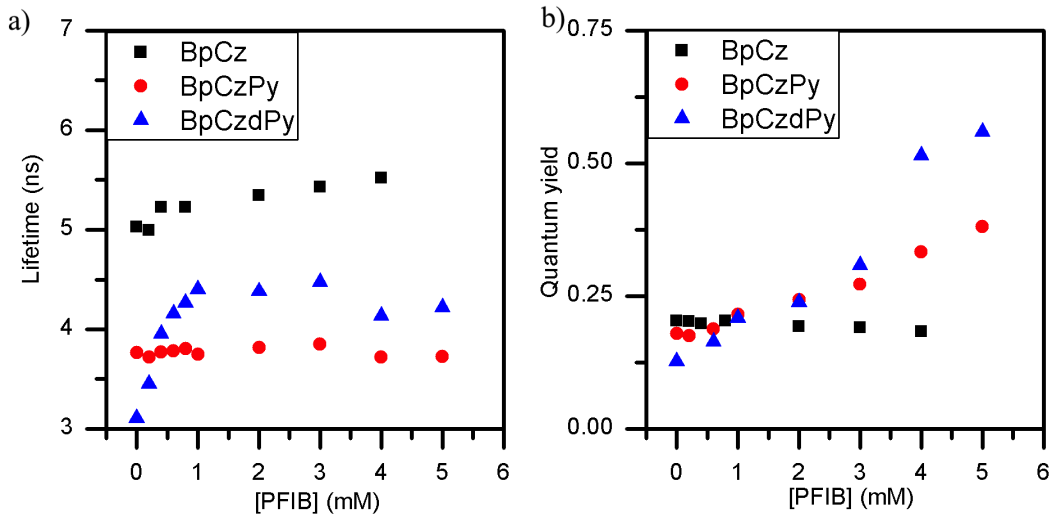

Figure 4.8 *Lifetimes and quantum yields of the titration series with pentafluoroiodobenzene. Samples were excited at 340 nm.*

the instrument resolution, whereas BpCzPy remains the same and BpCzdPy lifetime increases 1.5 ns. The excited-state lifetime is characteristic to a compound and changes in the lifetime indicate changes to the light emitting molecule. In this case, the changes are quite small and inconclusive.

The absorbance and emission measurement results were used to determine the changes in the emission quantum yield while titrating with PFIB. The emission quantum yields in these titration series are determined from one measurement point and are not as accurate as the linear fitting method. The effects of PFIB absorbance are visible in the BpCz emission spectra and it plays a role in the determination of the quantum yield as well. QY of BpCz has little to no change with the addition of PFIB. BpCzPy and BpCzdPy however, experience a significant increase in their quantum yields. BpCzPy quantum yield increases from 0.18 to 0.38 and BpCzdPy from 0.13 to 0.56 experiencing the greatest relative increase.

4.1.3 Phenol titration series

The results of titration series performed with using phenol are presented in Figure 4.9. At first, with a low concentration of phenol, there were no visible changes in the emission intensity of the samples. A significant increase in the phenol concentration of the solution resulted in a linear decrease in the emission intensity of all the samples. This is shown in Figure 4.9d where the relative change in the emission intensity is plotted against the added phenol concentration.

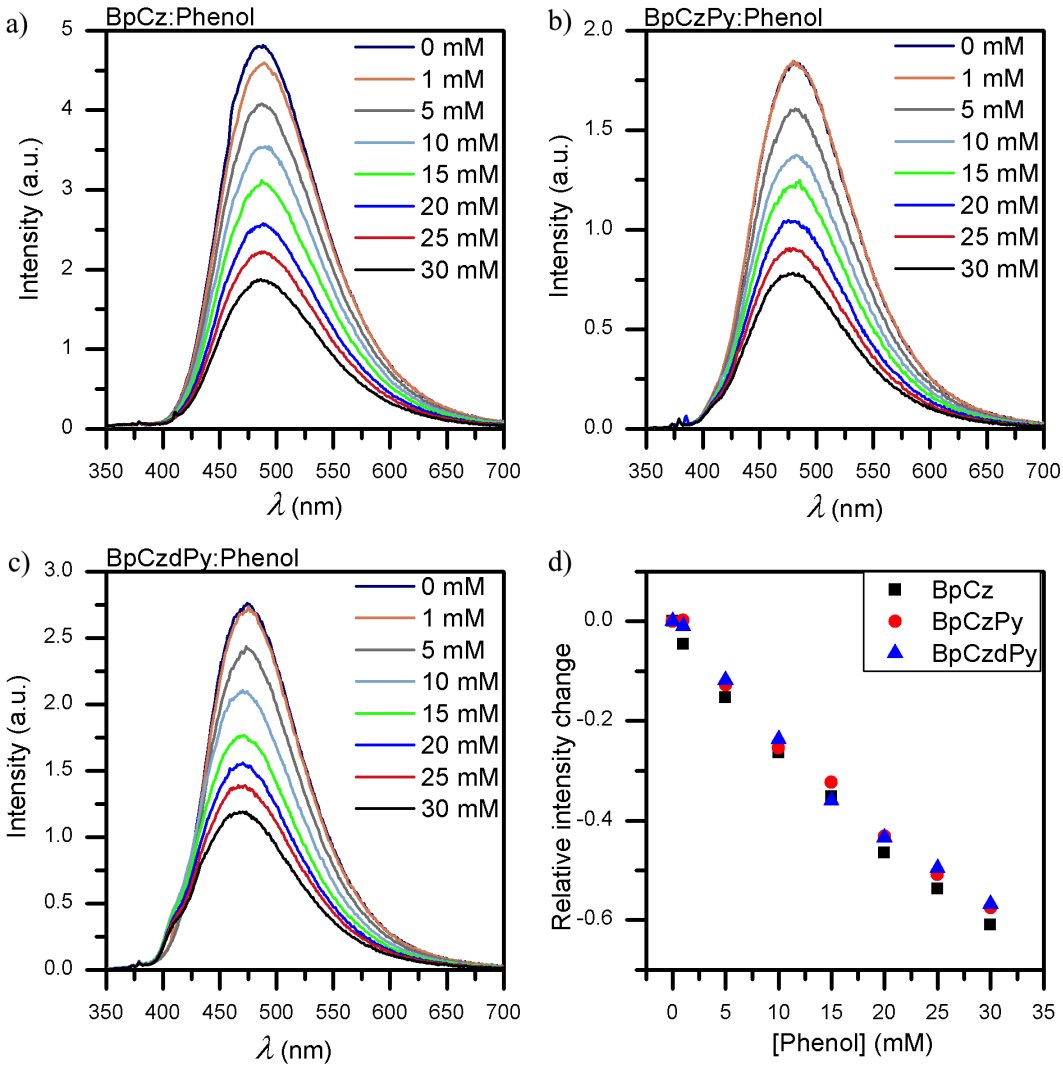

Figure 4.9 *The emission spectra of a) BpCz b) BpCzPy and c) BpCzdPy while titrated with phenol. Figure 4.9 d) presents the relative emission intensity change as a function of phenol concentration. Samples were excited at 340 nm.*

Phenol is a weak acid and its protonation is incomplete. It is more likely, that it will form hydrogen bonding with electron withdrawing atoms than form ionic interactions. The changes that occur during the addition of phenol are identical for all the samples. This indicates that hydrogen bonding with these compounds has no significant effects on the emission modulation. Also, no spectral shifts are visible with any of the samples. The decrease in the emission intensity of the samples is due to general solvent effects, rather than specific ones. Meaning that the addition of phenol to DCM solution changes the solvent properties to extent that results in a decrease in the emission intensity.

In the previous case, the absorbance of the PFIB lowered the emission intensity

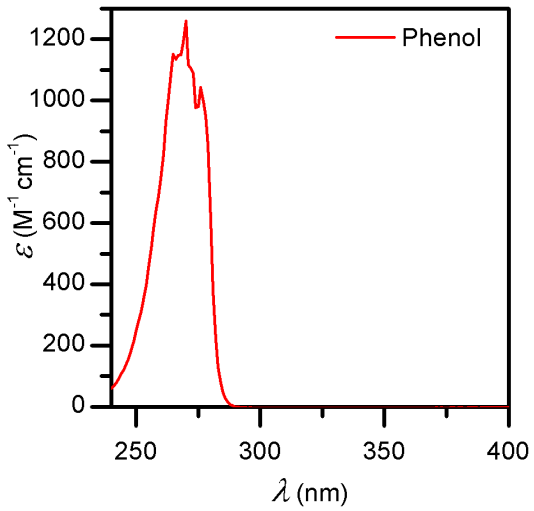

Figure 4.10 *The molar absorption coefficient (ϵ) of phenol as a function of wavelength (λ)*

with increasing PFIB concentration. Phenol however, does not absorb light at the excitation wavelength 340 nm as do the carbazole derivatives, and the decrease in the emission intensity is not affected by that. The molar absorption coefficient of phenol is presented in Figure 4.10 as a function of wavelength.

4.1.4 Benzenesulfonic acid titration series

Benzenesulfonic acid is a strong acid and the effects observed in the titration series are presumably from the protonation of the carbazole derivatives. BpCz has a carbonyl group which can be protonated, whereas BpCzPy and BpCzdPy have an additional one or two pyridyl groups with electron lone pairs. The changes in the absorbance of the samples while titrating with BSA, are presented in Figure 4.11.

The addition of BSA to BpCz solution seems to have little to no effect on the absorbance. However, absorption spectra of BpCzPy and BpCzdPy change significantly. BpCzPy has three isosbestic points at 308, 327 and 354 nm. The changes in the absorption bands are indicated with arrows in the figure. After BSA achieves 20 μM concentration, the changes in the spectrum are less significant. Similar trend occurs with BpCzdPy. It has one isosbestic point at 340 nm, absorption bands at 260, 300 and 325 nm decrease, whereas bands at 348 and 380 nm increase while the BSA concentration increases.

The results of the emission measurements of the titration are presented in Figure 4.12. BpCz shows a slight decrease in the emission intensity. BpCz has only

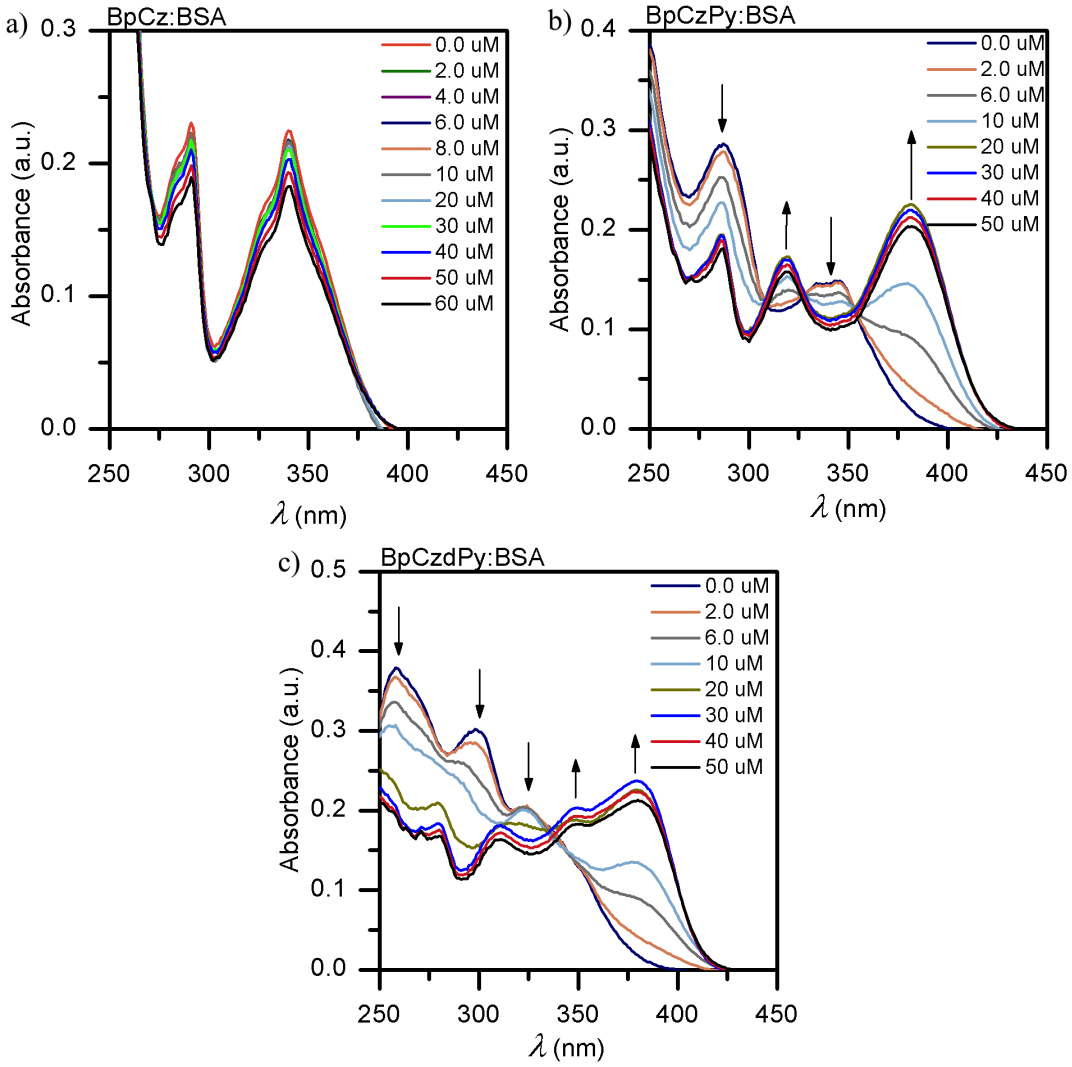

Figure 4.11 *Absorbances of the titration series with benzenesulfonic acid.*

the benzophenone carbonyl which is available for protonation, whereas BpCzPy and BpCzdPy have also pyridyl groups. The interaction observed in the case of BpCz is most likely due to changes in the solvent or hydrogen bonding to the carbonyl group. Although, with phenol titration series, no effects could be associated with hydrogen bonding.

In the case of the pyridine samples, the emission intensity increases significantly. The increase in the emission intensity is due to intramolecular charge transfer in the carbazole derivatives. For BpCzPy, the emission intensity increases until the BSA concentration reaches 20 μM. At this point, the concentration is twice the concentration of BpCzPy. The protonation of the pyridyl group induces the first increase of the emission intensity up to 10 μM concentration of BSA. At this point, all the pyridyl groups are protonated and the additional increase in the emission

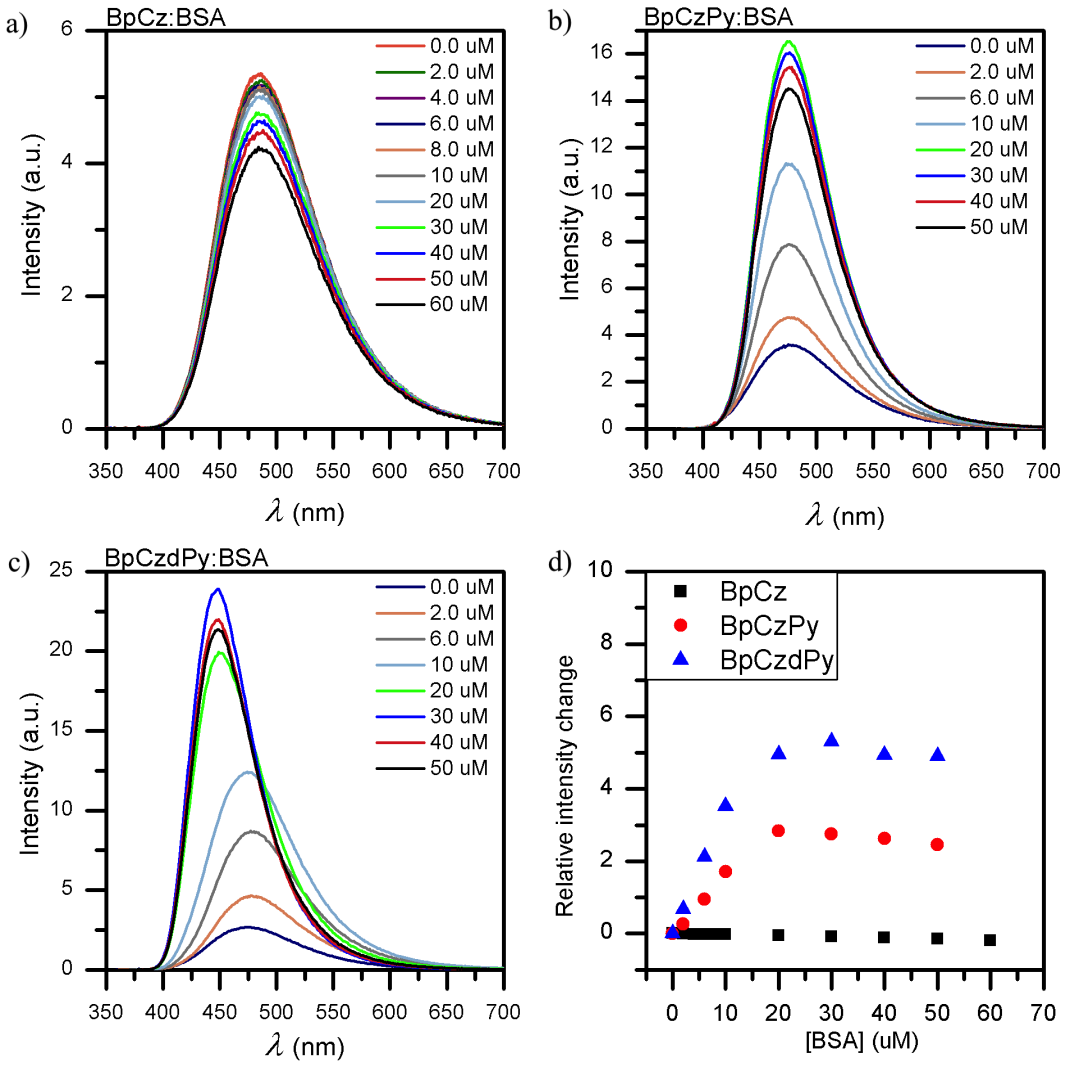

Figure 4.12 *Emission intensities of the titration series with benzenesulfonic acid. Figure d) presents the integrated relative emission intensity change. Samples were excited at 340 nm.*

intensity is due to BSA interaction with the carbonyl group. Without the pyridyl group, the interaction with the carbonyl decreases emission intensity, but with the protonated pyridyl, the emission intensity increases significantly. This might be due to a solvation effect on the carbonyl, which is decreased after a charge transfer induced by the protonation of the pyridyl group.

BpCzdPy experiences even more significant increase in the emission intensity until BSA concentration reaches 30 μM. At this point, both of the pyridyl groups are protonated and the emission intensity is increased even further because of BSA interaction with the carbonyl. In case of PFIB, it shows no saturation even though the used concentration goes up to five hundred times the concentration of the carbazole

derivative, but perhaps with larger concentrations the saturation would occur. BSA however, does show saturation, and the emission intensity increase is stoichiometric depending on how many pyridine and carbonyl groups the molecule possesses. With PFIB, there is no resemblance to stoichiometry in the relative integrated emission intensity change. BpCzdPy emission also shows a blue-shift of 50 nm, which is twice as large as for the PFIB. The effects of ionic interactions are significantly higher with very low concentrations in comparison with the halogen-bond-assisted emission modulation. Using 10 μM concentration of the benzenesulfonic acid, which is the initial concentration of the carbazole, we obtain similar results as with PFIB using five hundred times larger concentration.

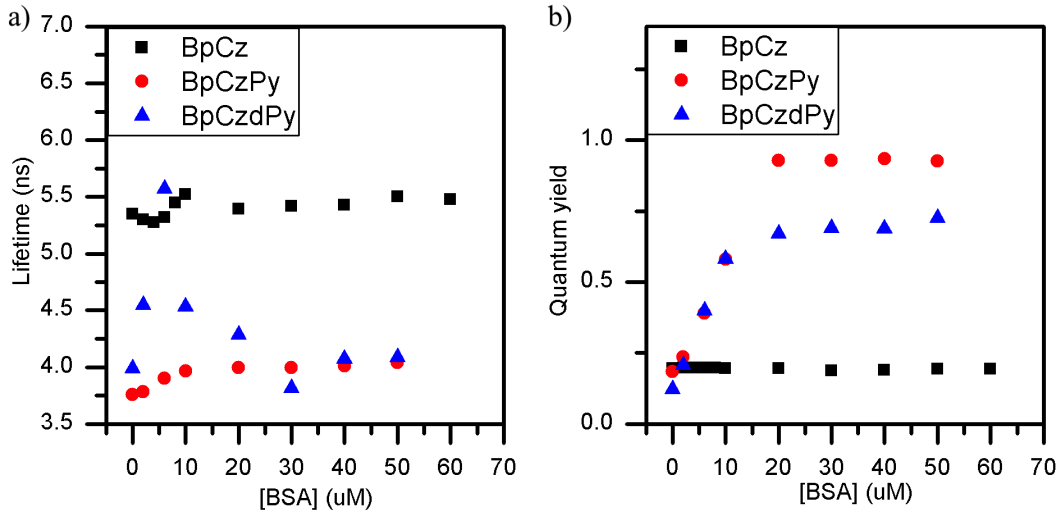

Figure 4.13 *Lifetimes and quantum yields of the titration series with benzenesulfonic acid. Samples were excited at 340 nm.*

Lastly, Figure 4.13 presents the changes in the longest component of the excited-state lifetime and quantum yield of the samples. BpCz experiences no changes in the lifetime or the emission quantum yield. BpCzPy has an increase of 0.5 ns in the excited-state lifetime and extremely high increase in the emission quantum yield from 0.18 to 0.93. BpCzdPy has also a significant increase in the quantum yield from 0.12 to 0.73. Lifetimes with both components and their percentages are presented in the Appendix A.

4.1.5 Pyridine titration series

The absorption spectra of the carbazole iodine derivatives titrated with pyridine are presented in Figure 4.14. The absorbance of BpCz increases below 300 nm with the addition of pyridine. For BpCzI, the case is similar, but there is also a slight increase in the absorption band around 340 nm. BpCzdI has two significant bands at 300 and 340 nm, which are both increased with the addition of pyridine to the solution.

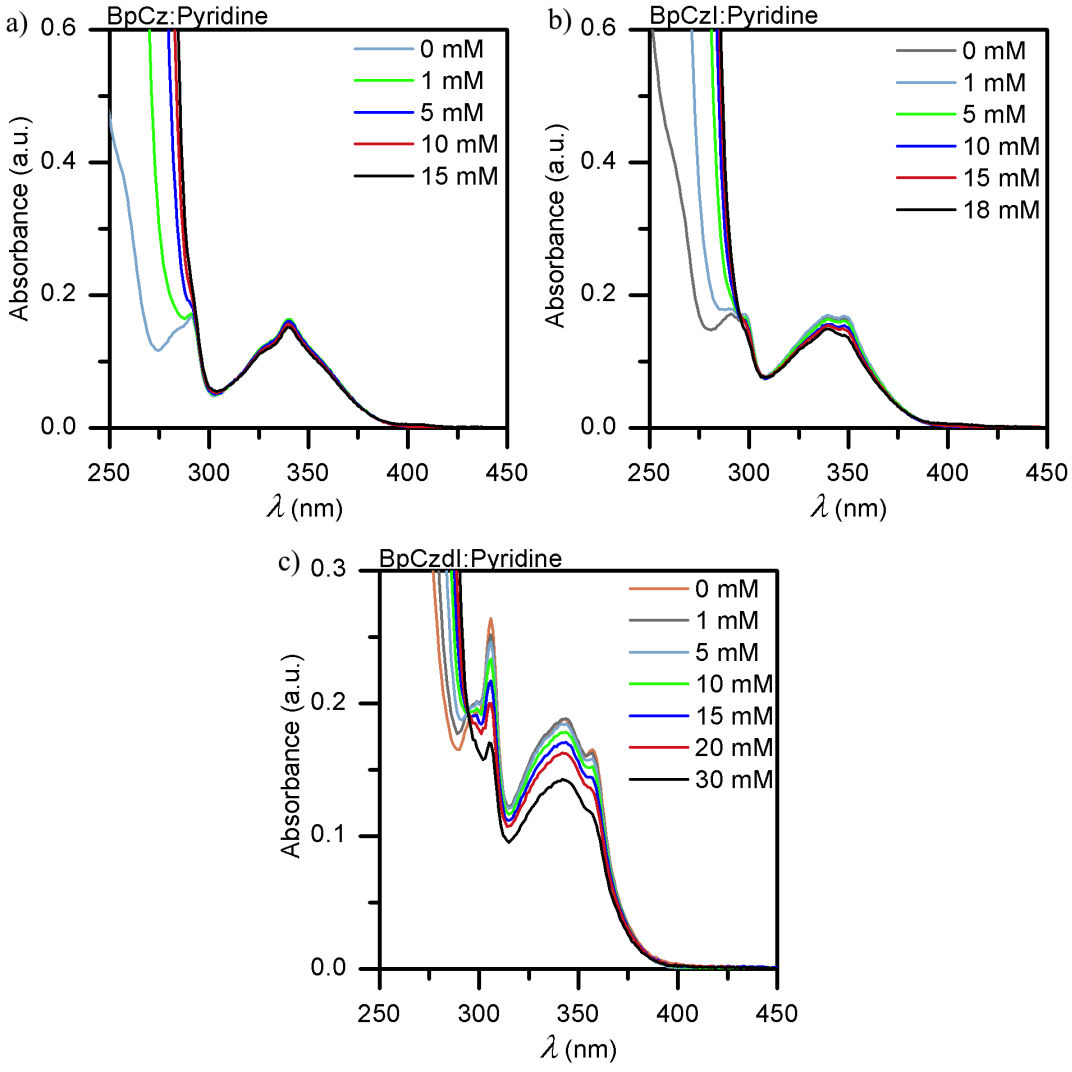

Figure 4.14 *Absorbances of the titration series with pyridine.*

The results of the emission measurements are presented in Figure 4.15. The emission intensity of BpCz decreases slightly with the increasing pyridine concentration. The changes are minor and due to general solvent effects. In the case of BpCzI, the emission intensity increases as pyridine concentration increases. This is most likely

due to halogen bonding. In this case, the BpCzI is the halogen bond donor and the added pyridine acts as an acceptor. A similar increase in the emission intensity of BpCzdI can be observed. In contrast to previous cases, the relative intensity change is greater for BpCzI than BpCzdI. None of the cases show saturation and the halogen bonding seems to have a weak effect on the intensity. The relative emission intensities are presented in Figure 4.15 d.

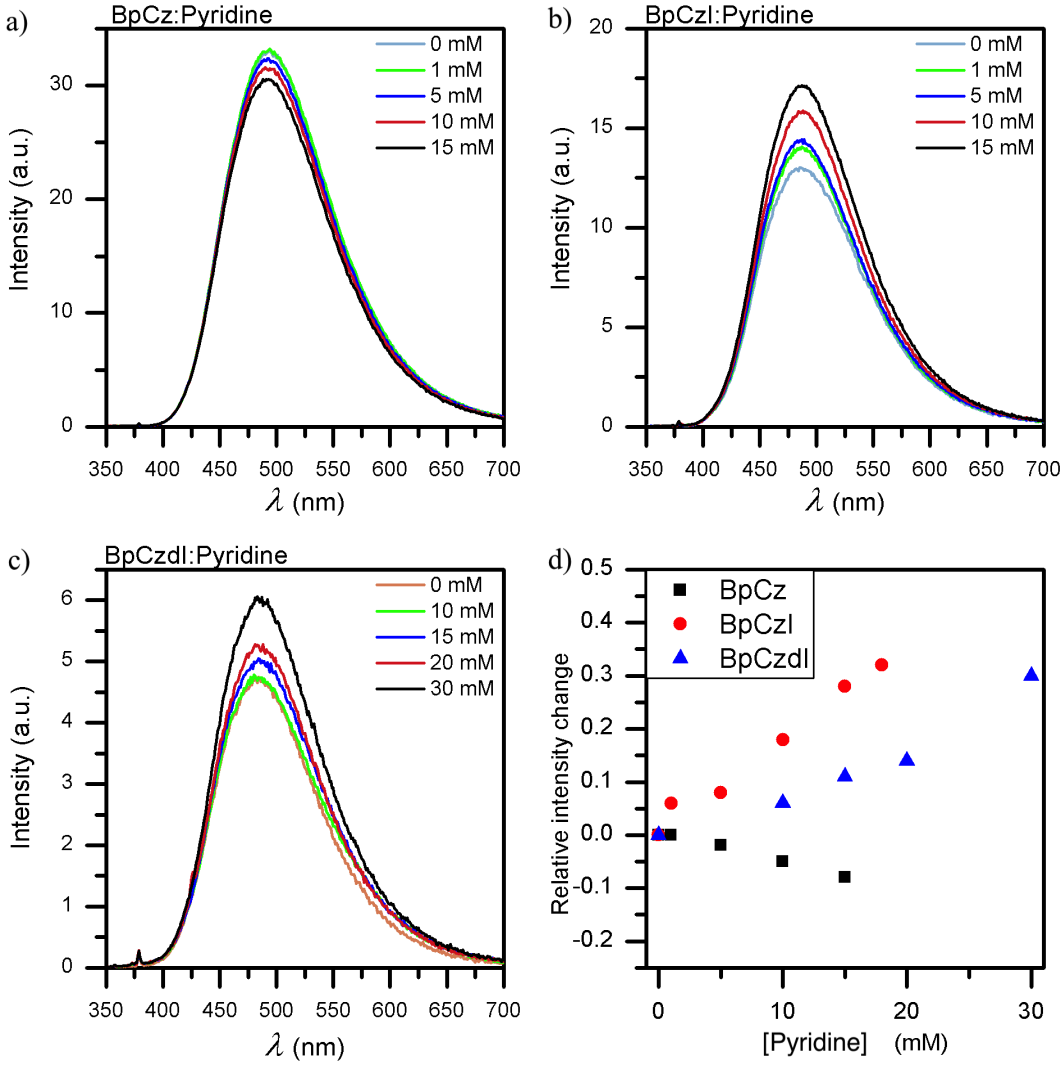

Figure 4.15 *Emission intensities of the titration series with pyridine. Samples were excited at 340 nm.*

The changes in the emission quantum yields and lifetimes of the samples are presented in Figure 4.16. The lifetime of BpCz decreases only 0.2 ns, which approaches the resolution of the TCSPC system. The quantum yield of BpCz has no change during the titration. For BpCzI, lifetime decreases 0.5 ns and the quantum yield increases 0.03 units. For BpCzdI, these values increase approximately 0.8 ns and 0.02 units. The lifetimes of the samples are also presented in a table in Appendix A.

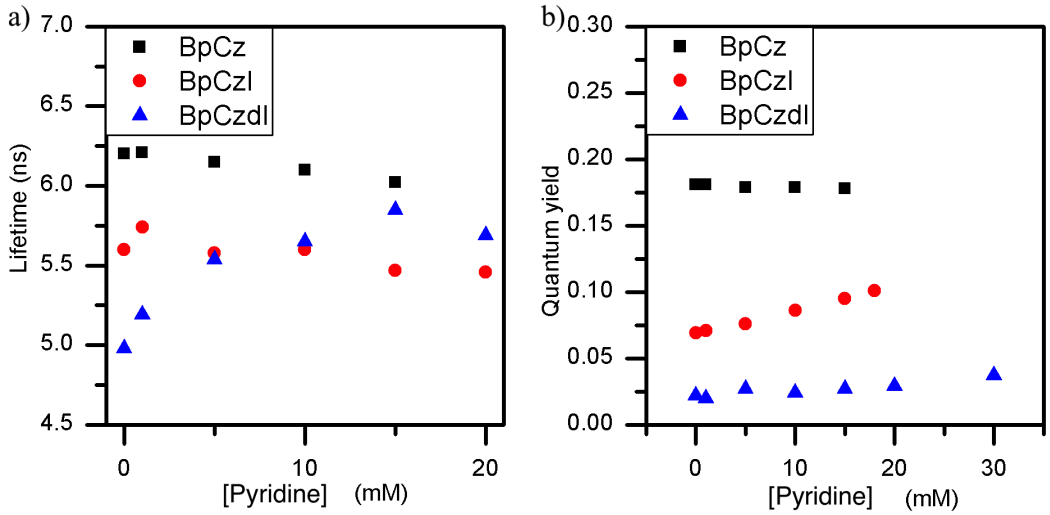

Figure 4.16 *Lifetimes and quantum yields of the titration series with pyridine. Samples were excited at 340 nm.*

From these results, one can determine that the benzophenone carbazole derivatives are much stronger halogen bond acceptors than they are donors. If we were to use iodoasetylene instead of iodine in the carbazole derivatives as was initially planned, we would have had a stronger halogen-bond donor and most likely obtained greater changes in the results. But unfortunately, the synthesis of this compound turned out to be difficult. Still, the protonation shows most significant interaction resulting in an extremely high increase in the emission intensity.

4.2 Non-covalent bonding in films

The pyridine compounds were characterized both in a reference matrix (PS) as well as hydrogen bond donor matrix (PVPh). The characterization of the films was done using 1 mol-% carbazole concentration for all the samples. Absorbance and emission spectra of BpCz and BpCzPy are presented in Figure 4.17.

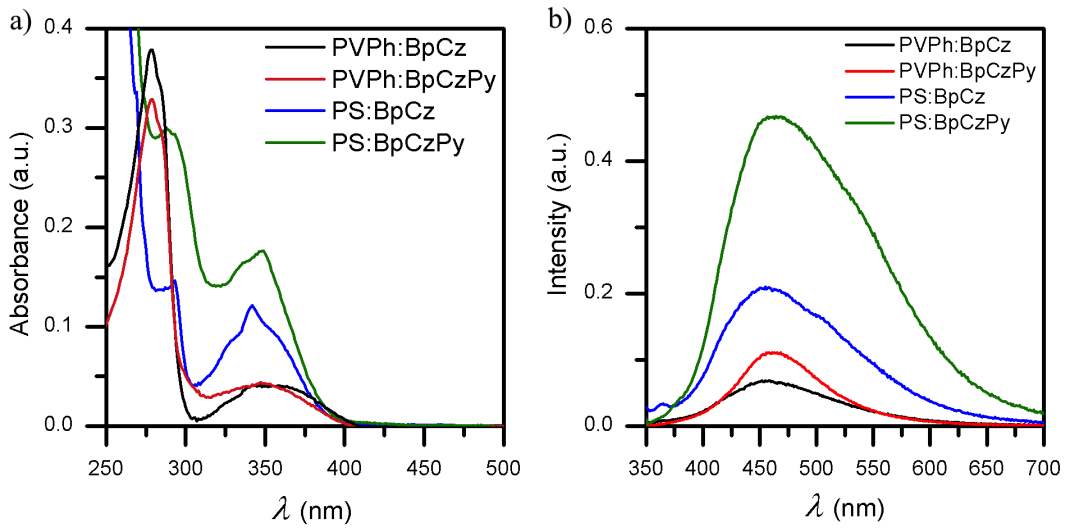

Figure 4.17 *Absorbance and emission intensities of BpCz and BpCzPy in PS and PVPh films. Samples were excited at 340 nm.*

All the samples absorb light in the UV region of the spectrum. In both cases, the spectrum displays features characteristic for the polymer matrix that are similar for BpCz and BpCzPy. Also, in both polymers, the absorbance of BpCzPy is higher than BpCz. In the case of the pyridine sample, the absorbance is more efficient in the reference polymer than the hydrogen bond donor.

The same trend continues in the emission spectra. The PS samples have stronger emission intensities than PVPh samples. Contrary to the solutions, BpCzPy has also higher emission intensities in both PS and PVPh samples than BpCz.

The iodine samples were characterized in PS and P4VP polymer matrices. P4VP was presumed to act as a halogen bond acceptor and the carbazole derivatives as halogen bond donors. The absorbance and emission spectra of the iodine compounds are presented in Figure 4.18. P4VP samples have very low absorbances at the excitation wavelength (340 nm), though experience relatively high emission intensities. In P4VP, BpCzI has higher absorbance and emission than BpCzdI. In PS samples, both absorbance and emission are nearly identical for BpCzI and BpCzdI. Lower BpCzdI absorbance and emission might be due to the worse solubility of BpCzdI to

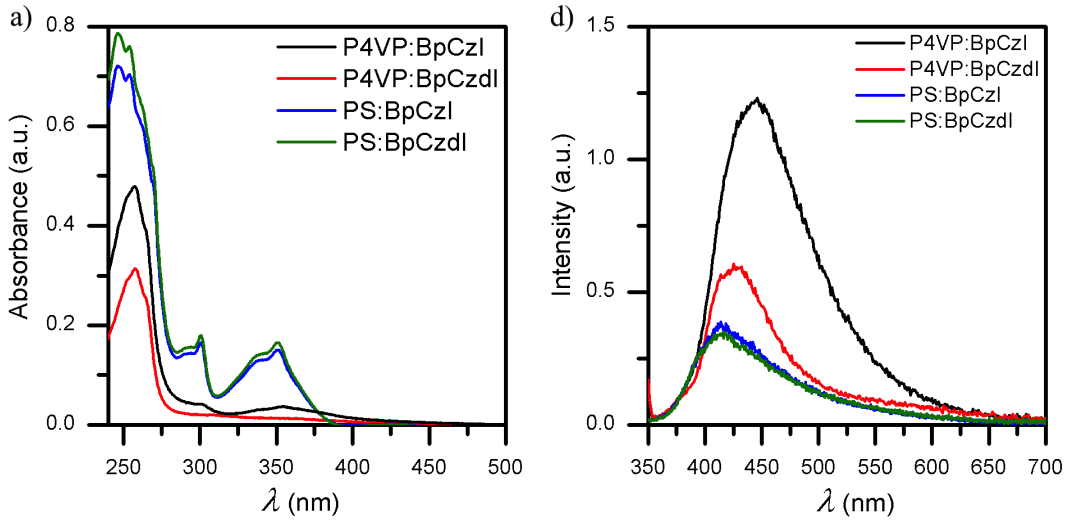

Figure 4.18 *Absorbance and emission intensities of BpCzI and BpCzdI in PS and P4VP films. Samples were excited at 340 nm.*

polymer solutions.

Overall, the halogen bonding seems to affect the polymer-chromophore complex, since the very low absorbances result in relatively high emission intensities, even though the heavy-atom effect and oxygen quenching presumably reduce the fluorescence.

4.2.1 Concentration series of thin films

Similar films that were described in the previous section were prepared as a concentration series to further study the effect of non-covalent bonding to the polymer matrix. Figure 4.19 presents the absorption and emission intensities of BpCz and BpCzPy in 2 to 40 mol-% concentrations relative to the PVPh concentration. The absorbance of both BpCz and BpCzPy increase linearly with the increasing chromophore concentration with few deviations. In both cases, while the chromophore concentration increases, the features in the spectra become more defined. The linearity of the increasing absorbance can be seen from Figure 4.20.

The emission of the BpCz:PVPh samples maintains its linear increase. It experiences a slight red-shift of 17 nm until the 15 mol-% concentration, and then the emission is shifted to lower wavelengths, the final maximums being 459, 447 and 445 nm. A similar occurrence can be observed for the BpCzPy, except that there is no significant red-shift. For BpCzPy, the emission intensity no longer follows the linear form but shows more of a saturation (Figure 4.20).

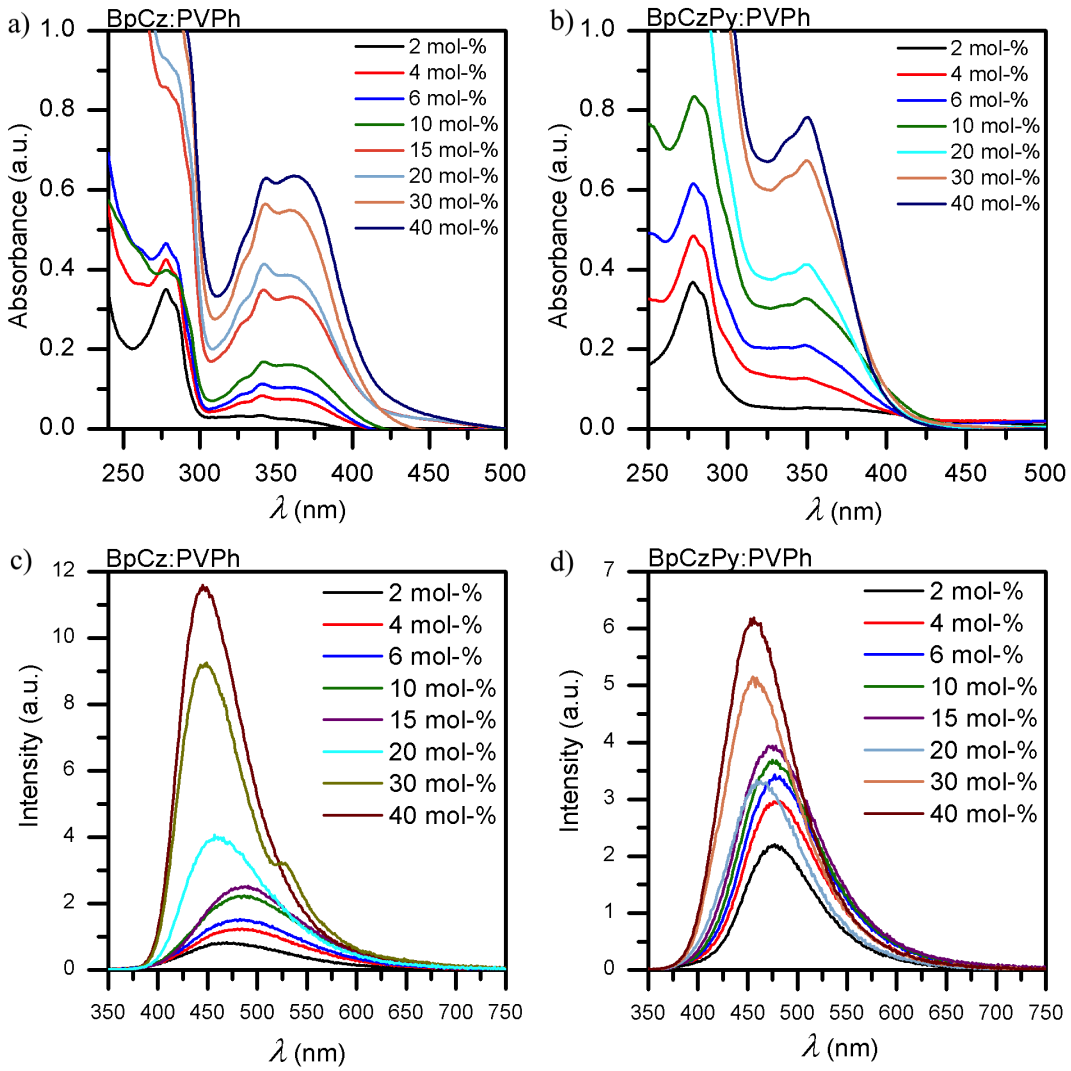

Figure 4.19 *Absorbance and emission intensities of the concentration series of a) BpCz and b) BpCzPy in PVPh films. Samples were excited at 340 nm.*

A similar concentration series was performed for the iodine compounds. The results of the series are presented in Figure 4.21. The shape of the absorption spectra of BpCzI produces distinct features belonging to the BpCzI while the concentration increases. At 20 mol-% concentration, the absorbance suddenly drops due to phase separation and keeps getting lower with increasing BpCzI concentration. Similar effects can be expected for the BpCzdI, but due to solubility issues, this saturation point was not obtained.

The emission of the samples follows the same trend as the absorbance. For BpCzI, it increases until 10 mol-% concentration, experiences a 15 nm blue-shift and decreases while the concentration increases. Overall, the emission of the iodine compounds is lower than the pyridine compounds in both solution and solid-state. The results of

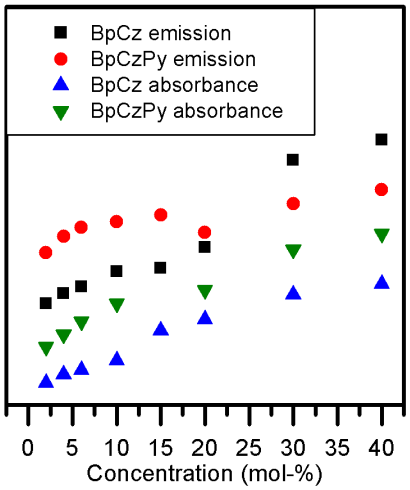

Figure 4.20 *The changes in the absorbance and integrated emission intensities during the concentration series. The results are scaled to fit into the same figure.*

the higher concentration films might not be reliable, since there was visible phase separation at least in samples 20-40 mol-% in the case of BpCzI. For BpCzdI, all the samples showed phase separation. When the sample shows phase separation, the film is no longer homogenous and the measurement position can significantly affect the result.

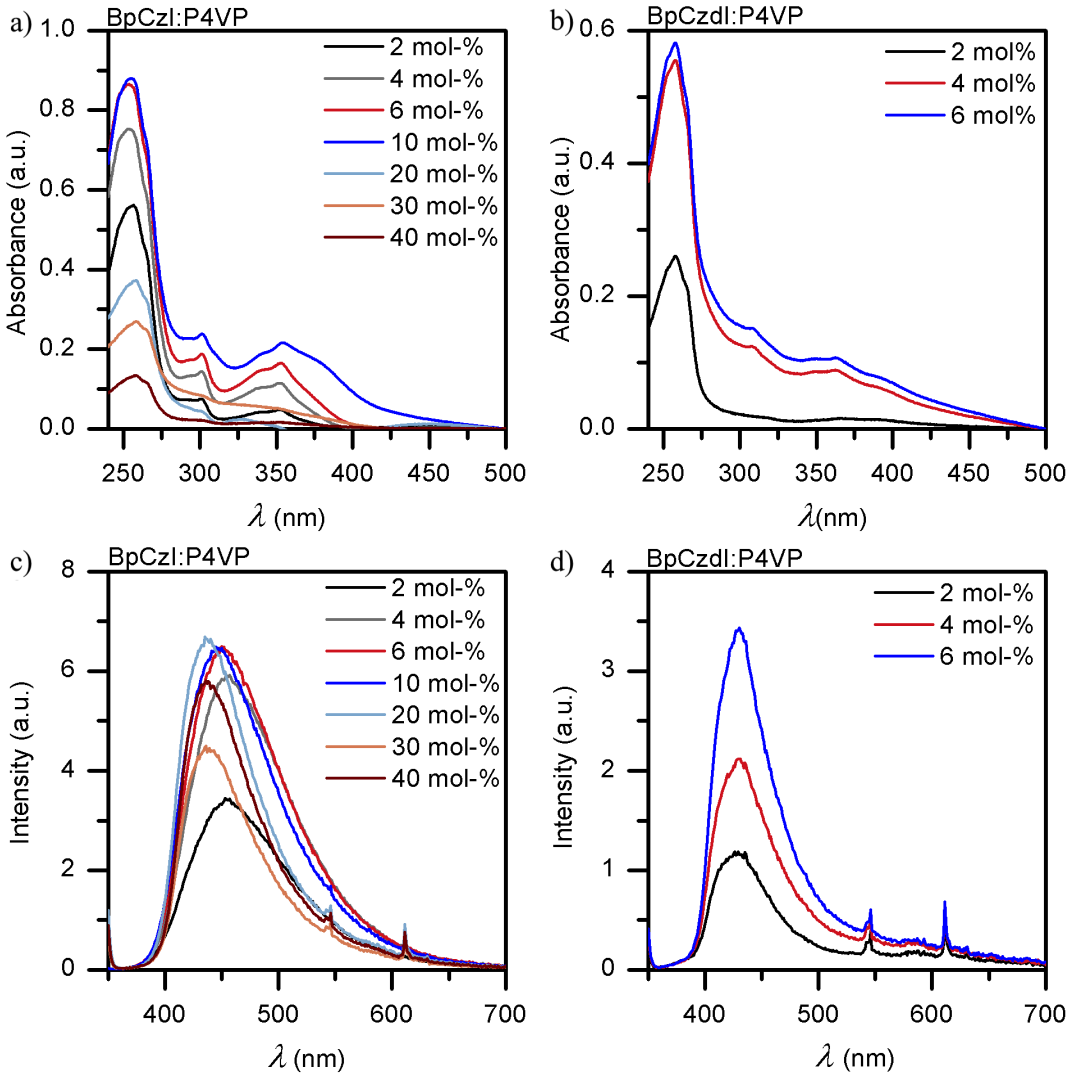

Figure 4.21 *Absorbance and emission intensities of the concentration (mol-%) series of a) BpCzI and b) BpCzdI in P4VP films where. Samples were excited at 340 nm.*

Determination of film thickness using optical profilometer

Film thickness was studied using an optical profilometer. The 3D images of some of the films with different concentrations are presented in Figure 4.22. The measured samples were BpCz and BpCzPy samples from 2 to 20 mol-%.

In these images, blue represents the surface of the quartz substrate that was covered with a tape while spin-coating, the sudden rise (light green to red) is the solution that was packed against the edge of the tape and the green part is the surface of the film. From these 3D images, the thickness of the films can be determined to be from roughly 160 to 180 nm. Also several samples were measured using DHM to study their surface roughness. The results are presented in Figure 4.22d. The "spikiness"

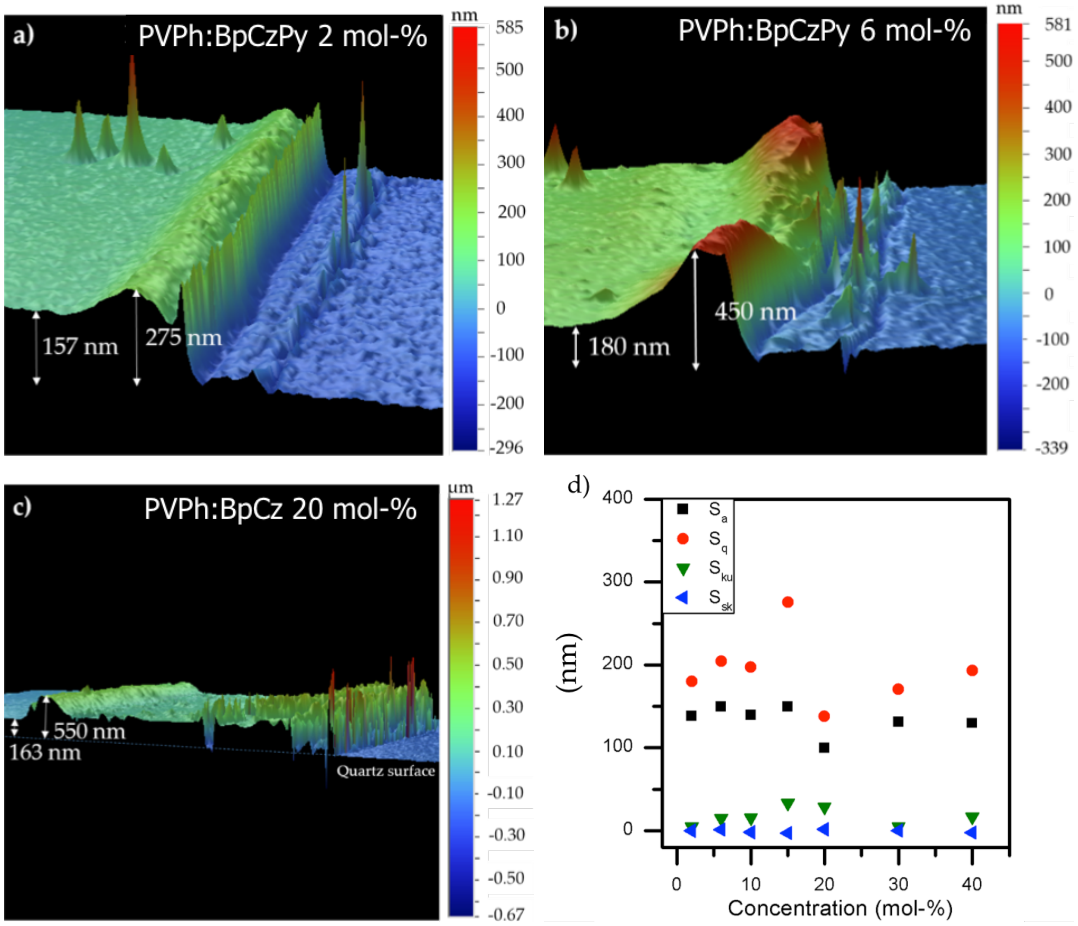

Figure 4.22 *Optical profilometer measurements of carbazole derivatives a) BpCzPy 2 mol-% b) BpCzPy 6 mol-% c) BpCz 20 mol-% d) results of DHM measurements of BpCzPy:PVPh samples with roughness parameters S_a, S_q, $S_k u$ and $S_s k$.*

and the asymmetry if the surfaces displays no significant variation between different samples. The average and root mean square values show more deviation, but no clear trend with the increasing concentration. From these measurements, no significant differences between samples with concentration differences can be determined.

4.2.2 Ionic interactions in films

Due to the results obtained from the titration series performed using BSA, poly(styrenesulfonic acid) films were prepared hoping to observe similar effects in the solid-state. The absorbances and emission intensities of PSS samples are presented in Figure 4.23. The BpCzPy:PSS samples, in comparison with PVPh samples (4.19), have broader absorbance starting as high as 500 nm. The intensity of the absorbance remains similar to that of PVPh samples. BpCz in PSS had only minimal light absorption.

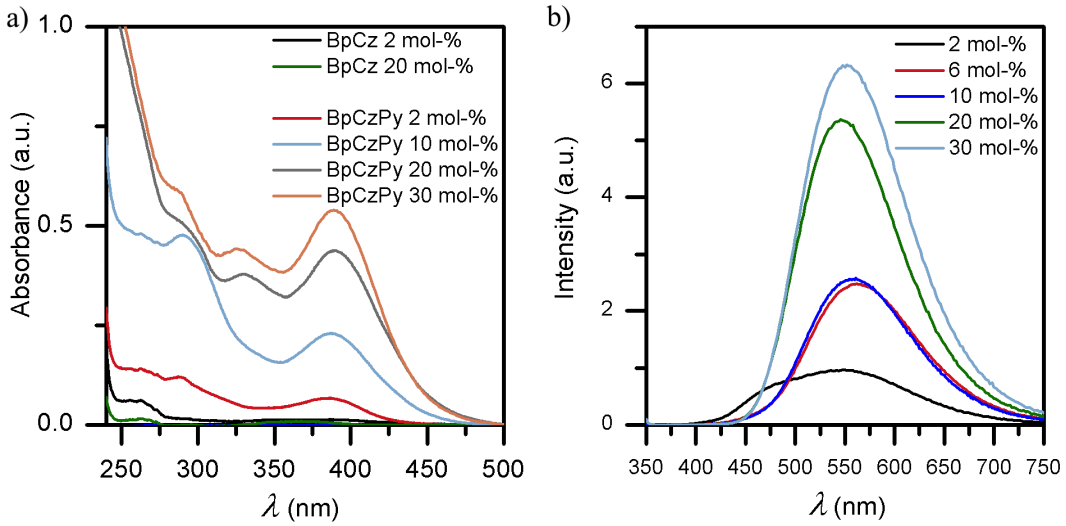

Figure 4.23 *Absorbance and emission intensities of BpCz and BpCzPy in PSS films. Figure b) presents only the emission intensities of BpCzPy in PSS at different BpCzPy concentrations (mol-%). Samples were excited at 340 nm.*

The emission intensities of the BpCz samples were not measured due to the very low absorbance. BpCzPy samples, however, present very high emission intensities compared to the previous films. The maximum varies from 560 nm to 550 nm, which is also roughly 100 nm higher in wavelength than PS or PVPh films. Unfortunately, the samples were not stable under illumination, but the emission intensity decreased rapidly while exciting the sample. Lifetimes of the PSS concentration series are presented in Table 4.2.

Table 4.2 *Lifetimes (ns) of PSS samples with various BpCzPy concentrations (mol-%).*

Concentration (mol-%)	BpCzPy		
	τ_1	τ_2	τ_3
2	18.8 (25%)	4.4 (34%)	1.1 (41%)
6	14.9 (15%)	4.6 (32%)	1.0 (53%)
10	15.1 (16%)	4.1 (36%)	0.8 (48%)
20	15.8 (21%)	5.2 (36%)	1.1 (43%)
30	14.2 (17%)	4.4 (38%)	1.1 (45%)

The longest component of the lifetime of the PSS samples decreases with the increasing chromophore concentration. The second and third components remain relatively the same during the concentration increase.

Stability studies in solid-state

PSS samples showed rapid degradation under illumination, so the effect was further studied by performing various measurements with a few samples. In Figure 4.24, the degradation process is illustrated. Figure 4.24 presents several measurements performed in 30 minutes under continuous irradiation. The starting intensity was 200 000 counts/s, from which the intensity decreased 60 % during the first 30 minutes of irradiation.

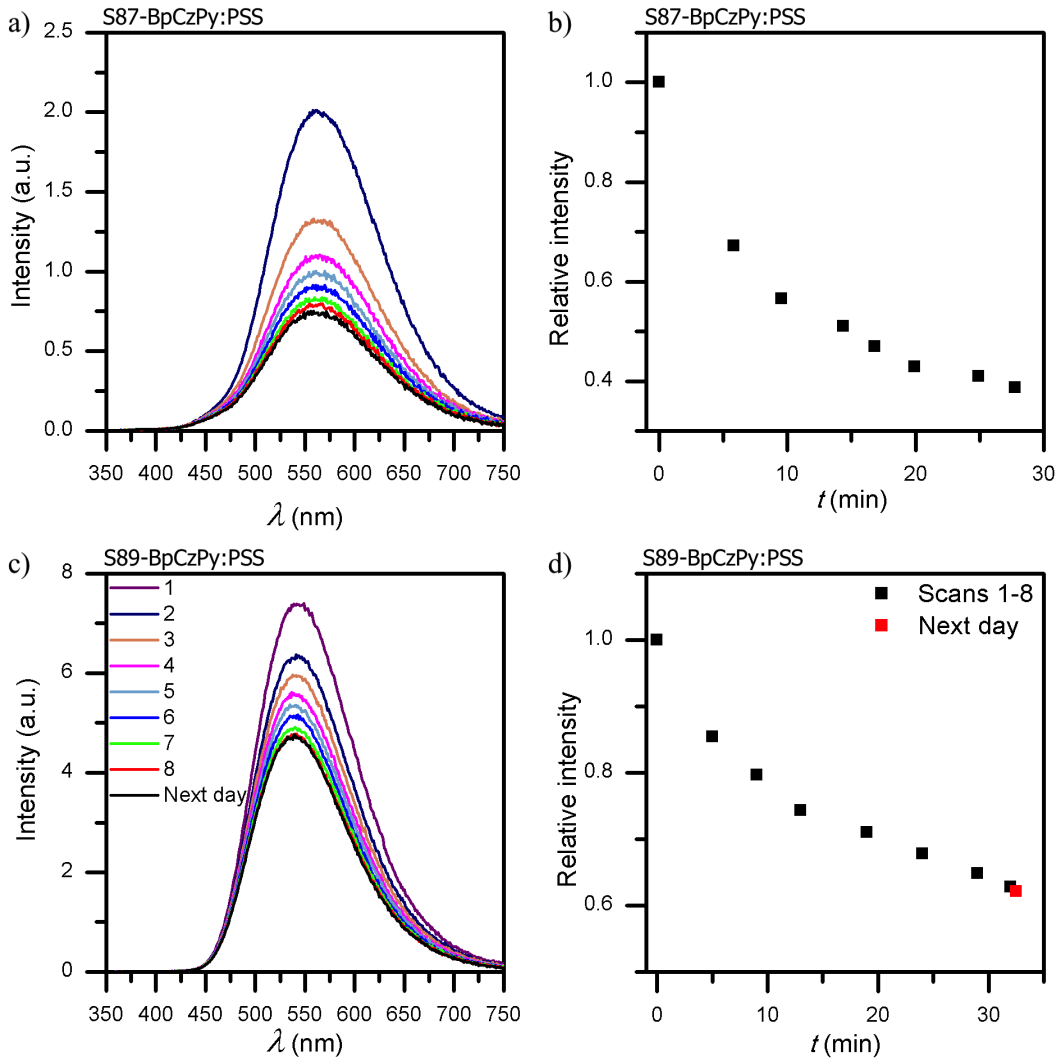

Figure 4.24 *Stability studies of PSS samples. a) presents the change in emission intensity of the sample under continuous irradiation and b) displays the same set of measurements as a function of time. c) and d) presents the same measurements for a different sample and d) also presents the value of the emission intensity after a relaxation until the next day. Samples were excited at 340 nm.*

The sample S89-BpCzPy:PSS was excited using 340 nm light and several emission

scans were measured keeping the sample under continuous irradiation. After this, the sample was left in the dark chamber overnight the ensure same measurement position and another emission scan was measured. The decrease in the emission intensity is described in Figure 4.24 d. The emission intensity neither returns to its initial value even after relaxation overnight nor does it decrease.

The optical properties of the sample are only decreased when the sample is under illumination. This suggests that the degradation process is due to the excitation of the sample. The sample was further studied to determine a reason for the photodegradation performing absorption and lifetime measurements. These results remained the same during 30 minutes of irradiation. The fact that the absorbance of the sample remains the same, even though the emission intensity decreases, suggests that the change occurs in the excited state of the sample only. Though, from the lifetime measurements, it was determined that the excited-state lifetime remained the same. It could also be that the excitation sources of the transient absorption spectrophotometer and the laser of the TCSPC system were not as powerful as the fluorimeter excitation source to study the degradation.

The sample was also studied using Fourier transform infrared spectroscopy (FTIR) to see possible structural changes before and after illumination, but the results remained the same. The IR spectra of the sample before and after irradiation are presented in Appendix B.

5. CONCLUSIONS AND OUTLOOK

Organic phosphorescent emitters are rare and usually based on toxic organometallic materials. This thesis investigates carbazole-based non-covalent bond acceptor and donor molecules as possible blue-light emitters with possibilities to even modulate the emission wavelength and intensity by non-covalent complex formation. The modulation of emission is affected by non-covalent bonding between the emitter and an additive compound. The effect of this modulation was studied both in solution and polymer-chromophore matrices.

The main focus of this thesis was to study the emission modulation of carbazole derivatives using non-covalent bonding. Carbazole is known as highly emitting material commonly used in blue-light emitting devices. Here, benzophenone-carbazole was used as a reference compound and two compounds with pyridyl substituents were characterized as HB and XB acceptors. In addition to that, two compounds with iodine substituents were characterized as XB donors. Having one or two substituents enabled to distinguish the extent of the effect induced by non-covalent bonding. All the compounds were characterized using absorption and emission spectroscopy as well as TCSPC.

The effects of non-covalent bonding to the carbazole derivatives were most clearly observed in solution. Halogen bonding to the carbazole derivatives, using pyridine compounds as XB acceptors resulted in a significant increase in the emission intensity of the emitter. The halogen-bond induced intramolecular charge transfer is enhanced by the electron-rich carbazole core by increasing the electron density of the pyridine acceptor moieties. Similar results with even more significant effects could be observed with ionic interactions where pyridine compounds were protonated. These experiments also resulted in significant increases in emission quantum yields, BpCzPy achieving 0.93 QY due to protonation. Both pyridine compounds could be exposed to emission color change upon complexation with HB and XB donors. A weak hydrogen bonding to these pyridine compounds did not affect the emission properties.

The iodine compounds were studied as XB donor molecules in a similar fashion.

This also resulted in emission intensity increase, but much less significant than with the pyridine compounds. From these solution experiments, it was concluded that the pyridine compounds are much stronger HB and XB acceptors than the iodine compounds are XB donors. Also, the emission intensity can be effectively modulated through halogen bonding and very strong hydrogen bonding or protonation in solution.

The compounds were studied as possible materials for tunable light emitting devices and therefore were also characterized in the solid state. In the solid state, the effects of non-covalent bonding led to similar results as in solution, but the effects were not as distinct. The effect of protonation was also studied in solid-state with poly(styrenesulfonic acid) polymer. Again, it conveyed similar results as the solution studies, but unfortunately, these films were not photostable. Overall, the film thicknesses had only slight variation and were relatively planar using a spin-coating method.

The results of this study suggest that halogen bonding increases the emission intensity of organic compounds due to halogen-bond induced charge transfer and can be used to tune the luminescence of organic compounds. Also, protonation of the compound can be used to modify the charge distribution and enhance the emission intensity. The protonation is highly dependent on stoichiometry and the interactions are easier to predict than in the case of halogen bonding. In both cases, the emission wavelength can also be tuned by controlling the intermolecular interactions. These can also be used to increase the emission quantum yield of organic compounds.

The results of this study raise further interest to study the behaviour of organic compounds in solution and the changes in their luminescence induced by non-covalent bonding. This study could be taken further to perform more titration series using multiple acids with similar structures but various dissociation constants. In this way the process of protonation could be studied step by step. Additionally, X-ray crystallography could be used to confirm the presumptions drawn from these results. Halogen bonding could also be studied in similar way by varying the strength of the XB donor molecule.

BIBLIOGRAPHY

[1] Lakowicz, J. R., Principles of Fluorescence Spectroscopy, 2006, Springer, Maryland, USA.

[2] Mukherjee, S., Thilagar, P., Recent Advances in Purely Organic Phosphorescent Materials, Chem. Commun., 2015, 51, pp. 10988–11003.

[3] Cavallo, G., Metrangolo, P., Milani, R., Pilati, T., Priimagi, A., Resnati, G., Giancarlo, T., The Halogen Bond, Chem. Rev. 2016, 116, pp. 2478–2601.

[4] Wardle, B., Principles and Applications of Photochemistry, 2009, John Wiley & Sons, Ltd., United Kingdom.

[5] Engel, T., Reid, P., Physical Chemistry, 2006, Pearson Education Inc., San Francisco.

[6] Valeur, B., Berberan-Santos, M. N., Molecular Fluorescence, Principles and Applications, 2013, Wiley-VCH, Germany.

[7] Glossary of terms used in photochemistry (IUPAC Recommendations 1996), p. 2281.

[8] Gold Book, IUPAC, Delayed Fluorescence.

[9] Koziar, J. C., Cowan, D. O., Photochemical Heavy-Atom effects, Acc. Chem. Res., 1978, 11 (9), pp. 334–341.

[10] Clemens, O., Basters, M., Wild, M., Wilbrand, S., Reichert, C., Bauer, M., Springborg, M., Jung, G., Solvent effects on the absorption/emission spectra of an organic chromophore: A theoretical study, Journal of Molecular Structure: THEOCHEM, 866, 2008, pp.15–20.

[11] Díaz, M. S., Freile, M. L., Gutiérrez, M. I., Solvent effect on the UV/Vis absorption and fluorescence spectroscopic properties of berberine, Photochem. Photobiol. Sci., 2009, 8, pp. 970–974.

[12] Steed, J. W., Atwood, J. L., Supramolecular Chemistry 2nd ed., 2009, John Wiley & Sons, Ltd., UK.

[13] Buckingham, A. D., Del Bene, J. E., McDowell, S. A. C., The Hydrogen Bond, Chemical Physics Letters, 2008, 463, pp. 1–10.

[14] Steiner, T., The Hydrogen Bond in the Solid State, Angew. Chem. Int. Ed., 2002, 41, pp. 48–76.

[15] IUPAC. Compendium of Chemical Terminology, 2nd ed. (the "Gold Book"). Compiled by A. D. McNaught and A. Wilkinson. Blackwell Scientific Publications, Oxford (1997). XML on-line corrected version: http://goldbook.iupac.org (2006-) created by M. Nic, J. Jirat, B. Kosata; updates compiled by A. Jenkins. ISBN 0-9678550-9-8. https://doi.org/10.1351/goldbook.

[16] Desiraju, G. R., Ho, P. S., Kloo, L., Legon, A. C., Marquardt, R., Metrangolo, P., Politzer, P., Resnati, G., Rissanen, K., Definitions of the halogen bond (IUPAC Recommendations 2013), Pure Appl. Chem., 2013, Vol. 85, No. 8, pp. 1711–1713.

[17] Politzer, P., Lane, P., Concha, M., Ma, Y., Murray, J., An Overview of Halogen Bonding, J Mol Model, 2007, 13, pp. 305–311.

[18] Priimagi, A., Cavallo, G., Forni, A., Gorynsztein-Leben, M., Kaivola, M., Metrangolo, P., Milani, R., Shishido, A., Pilati, T., Resnati, G., Terraneo, G., Halogen Bonding versus Hydrogen Bonding in Driving Self-Assembly and Performance of Light-Responsive Supramolecular Polymers, Adv. Funct. Mater. 2012, 22, pp. 2572–2579.

[19] Salunke, J., Durandin, N. A., Ruoko, T-P., Candeias, N. R., Vivo, P., Vuorimaa-Laukkanen, E., Laaksonen, T., Priimagi, A., Halogen-Bond-Assisted Photoluminescent Modulation in Carbazole Based Emitter, Scientific Reports 8, 14431, 2018.

[20] Yan, D., Delori, A., Lloyd, G. O., Friscic, T., Day, G. M., Jones, W., Lu, J.,Wei, M., Evans, D. G.,Duan, X., A cocrystal strategy to tune the luminescent properties of stilbene-type organic solid-state materials, Angew. Chem. Int. Ed., 2011, 50, pp. 12483–12486.

[21] Bolton, O., Lee, K., Kim, H.J., Lin, K.Y., Kim, J., Activating efficient phosphorescence from purely organic materials by crystal design, Nat. Chem., 2011, 3 (3), pp. 205–210.

[22] Shi, L., Liu, H-Y., Shen, H., Hu, J., Zhang, G-L., Wang, H., Ji, L-N., Chang, C-K., Jiang, H-F., Fluorescence properties of halogenated mono-hydroxyl corroles: the heavy-atom effects, Journal of Porphyrins and Phthalocyanines, 13, 2009, No. 12, pp. 1221–1226.

[23] Kwon, M.S., Lee D., Seo S., Jung J., Kim J., Tailoring intermolecular interactions for efficient room-temperature phosphorescence from purely organic materials in amorphous polymer matrices, Angew. Chem. Int. Ed. Engl., 2014,13;53 (42) pp.11177–81.

[24] Zumdahl, S., Chemical principles, 2009, Houghton Mifflin Company, USA.

[25] Sultanova, N., Kasarova, S., Nikolov, I., Dispersion Properties of Optical Polymers, Acta Physica Polonica A, 2009, 116, pp. 585–587.

[26] Dubois J., Spitz, E., Properties and Applications of Polymers in Optics and Electrooptics, 1994, In: Prasad P.N. (eds) Frontiers of Polymers and Advanced Materials. Springer, Boston, MA.

[27] Pale, V. et al., Biomimetic Zinc Chlorin-poly(4-vinylpyridine) Assemblies: Doping Level Dependent Emission-Absorption Regimes, J. Mater. Chem. C, 2013, 1, pp. 2166–2173.

[28] Baroncini, M., Bergamini, G., Ceroni, P., Rigidification or Interaction-induced Phosphorescence of Organic Molecules, Chem. Commun. 2017, 53, pp. 2081–2093.

[29] Priimagi, A., Cattaneo, S., Ras, R. H. A., Valkama, S., Ikkala, O., Kauranen, M., Polymer-dye complexes: supramolecular route toward functional optical materials, Proc. SPIE 6192, Organic Optoelectronics and Photonics II, 61922U, 2006.

[30] Priimagi, A., Cattaneo, S., Ras, R. H. A:, Valkama, S., Ikkala, O., Kauranen, M., Polymer-Dye Complexes: A Facile Method for High Doping Level and Aggregation Control of Dye Moleucules, Chem. Mater. 2005, 17, pp. 5798–5802.

[31] Priimagi, A., Kaivola, M., Rodriguez, F. J., Kauranen, M., Enhanced photoinduced birefringence in polymer-dye complexes: Hydrogen bonding makes a difference, Applied Physics Letters, 90, 121103, 2007.

[32] South, C., Burd, C., Weck, M., Modular and Dynamic Functionalization of Polymeric Scaffolds, Acc. Chem. Res., 2007, 40, pp. 63–74.

[33] Rajamalli, P., Martir, D. R., Zysman-Colman E., Pyridine-functionalized carbazole donor and benzophenone acceptor design for thermally activated delayed fluorescence emitters in blue organic light emitting diodes, Journal of photonics for energy 2018, 8 (3).

[34] Kim, S. H., Cho, I., Sim, M. K., Park S., Park S. Y., Highly efficient deep-blue emitting organic light emitting diode based on the multifunctional fluorescent molecule comprising covalently bonded carbazole and anthracene moieties, J. Mater. Chem., 2011, 21, pp. 9139–9148.

[35] Adhikari, R. M., Mondal, R., Shah, B. K., Neckers, D. C., Synthesis and photophysical properties of carbazole-based blue light-emitting dendrimers, J. Org. Chem., 2007, 72 (13), pp. 4727–4732.

[36] Reig, M. et al., Easy accessible blue luminescent carbazole-based materials for organic light-emitting diodes, Dyes and Pigments, 2017, 137, pp. 24–35.

[37] IUPAC. Compendium of Chemical Terminology, 2nd ed. (the "Gold Book"). Compiled by A. D. McNaught and A. Wilkinson. Blackwell Scientific Publications, Oxford (1997). XML on-line corrected version: http://goldbook.iupac.org (2006-) created by M. Nic, J. Jirat, B. Kosata; updates compiled by A. Jenkins. ISBN 0-9678550-9-8. https://doi.org/10.1351/goldbook.

[38] Seppälä, J., Polymeeriteknologian perusteet, 1998, Hakapaino Oy, Helsinki.

[39] Tkachenko, N. V., Optical Spectroscopy, Methods and Instrumentation, 2006, Elsevier B. V.

[40] Hollas, M. J., Modern Spectroscopy, John Wiley and Sons, 2004, UK, 452 p.

[41] Albani, J. R., Fluorescence: Principles and Observables in Structure and Dynamics of Macromolecules: Absorption and Fluorescence Studies, 2004. Elsevier B.V.

[42] Lamb, C., and Zecchino, M., Wyko Surface Profilers Technical Reference Manual, 1999, Veeco, Metrology Group, USA, 151 p.

[43] Kemper, B., Langehanenberg, P., von Bally, G., Digital Holographic Microscopy A new Method for surface Analysis and Marker-Free Dynamic Life cell imaging, 2007 WiLEY-Vch Verlag Gmbh & co. KGaA, Weinheim.

APPENDIX A

Table 1 *Lifetimes of BpCz, BpCzPy and BpCzdPy with various PFIB concentrations (mM). The changes in the lifetime of the longest living component are also presented in Figure 4.8.*

[PFIB] (mM)	BpCz		BpCzPy		BpCzdPy	
	τ_1	τ_2	τ_1	τ_2	τ_1	τ_2
0	1.33 (14%)	5.03 (86%)	3.77 (76%)	1.62 (24%)	3.10 (36%)	1.63 (64%)
0.2	1.19 (14%)	4.99 (86%)	3.72 (77%)	1.46 (23%)	3.45 (33%)	1.65 (67%)
0.4	2.07 (17%)	5.22 (83%)	3.77 (77%)	1.42 (23%)	3.95 (33%)	1.68 (67%)
0.6	-	-	3.78 (78%)	1.42 (22%)	4.16 (37%)	1.72 (63%)
0.8	2.01 (16%)	5.23 (84%)	3.80 (80%)	1.37 (20%)	4.26 (44%)	1.71 (56%)
1	-	-	3.74 (83%)	0.86 (27%)	4.40 (51%)	1.74 (49%)
2	1.91 (19%)	5.35 (81%)	3.82 (83%)	1.38 (17%)	4.38 (63%)	1.64 (37%)
3	5.43 (80%)	1.77 (20%)	3.85 (83%)	1.58 (17%)	4.47 (70%)	1.80 (30%)
4	5.54 (79%)	1.63 (21%)	3.72 (89%)	0.57 (11%)	4.13 (43%)	2.18 (57%)
5	-	-	3.72 (93%)	1.11 (7%)	4.22 (27%)	2.39 (73%)

Table 2 *Lifetimes of BpCz, BpCzPy and BpCzdPy with various BSA concentrations (μM). The changes in the lifetime of the longest living component are also presented in Figure 4.13.*

[BSA] (μM)	BpCz		BpCzPy		BpCzdPy	
	τ_1	τ_2	τ_1	τ_2	τ_1	τ_2
0	5.35 (87%)	1.54 (13%)	3.76 (77%)	1.72 (23%)	3.99 (26%)	1.56 (74%)
2	5.30 (87%)	1.54 (13%)	3.78 (82%)	1.15 (18%)	4.55 (43%)	1.67 (57%)
4	5.27 (87%)	1.68 (13%)	-	-	-	-
6	5.32 (86%)	1.54 (14%)	3.90 (86%)	1.09 (14%)	4.57 (63%)	1.68 (37%)
8	5.45 (83%)	1.87 (17%)	-	-	-	-
10	5.52 (80%)	1.98 (20%)	3.97 (88%)	1.01 (12%)	4.53 (68%)	1.81 (32%)
20	5.39 (82%)	1.60 (18%)	4.0 (91%)	0.88 (9%)	4.28 (38%)	2.30 (62%)
30	5.42 (81%)	1.23 (19%)	4.0 (90%)	0.81 (10%)	3.81 (32%)	2.28 (68%)
40	5.43 (81%)	1.35 (19%)	4.01 (88%)	0.82 (12%)	4.07 (27%)	2.29 (73%)
50	5.50 (80%)	1.91 (20%)	4.04 (88%)	0.97 (12%)	4.09 (30%)	2.24 (70%)
60	5.48 (78%)	1.51 (22%)	-	-	-	-

Table 3 *Lifetimes of BpCz, BpCzPy and BpCzdPy with various pyridine (Py) concentrations (mM). The changes in the lifetime of the longest living component are also presented in Figure 4.16.*

[Py] (mM)	BpCz		BpCzPy		BpCzdPy	
	τ_1	τ_2	τ_1	τ_2	τ_1	τ_2
0	6.20 (66%)	0.98 (34%)	5.60 (25%)	0.70 (75%)	4.98 (2%)	0.43 (98%)
1	6.21 (66%)	0.97 (34%)	5.74 (25%)	0.72 (75%)	5.19 (4%)	0.43 (96%)
5	6.15 (66%)	0.94 (34%)	5.58 (27%)	0.67 (73%)	5.54 (4%)	0.44 (96%)
10	6.10 (67%)	0.95 (33%)	5.60 (31%)	0.70 (70%)	5.65 (5%)	0.47 (95%)
15	6.02 (66%)	0.99 (34%)	5.47 (35%)	0.71 (65%)	5.85 (6%)	0.49 (94%)
20	-	-	5.46 (41%)	0.73 (59%)	5.69 (8%)	0.49 (92%)
30	-	-	-	-	5.49 (13%)	0.52 (87%)

APPENDIX B

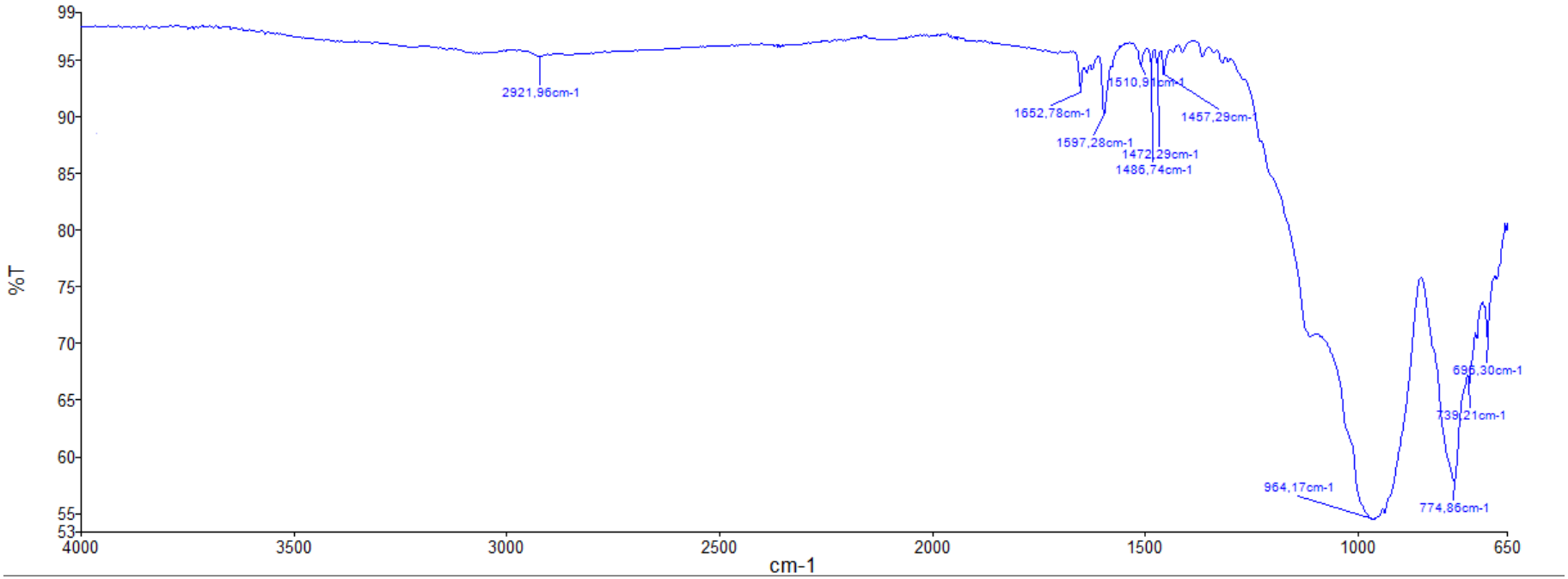

Figure 1 *IR spectrum of BpCzPy:PSS sample before illumination*

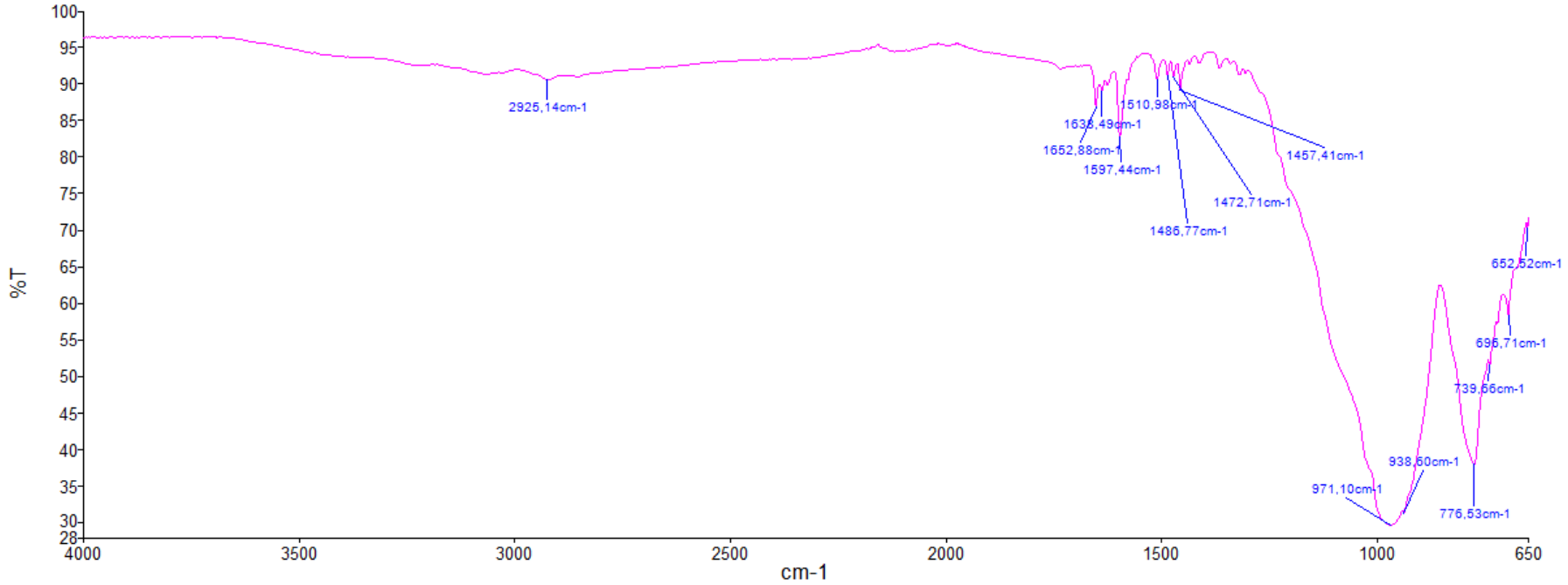

Figure 2 *IR spectrum of BpCzPy:PSS sample after 30 minutes of illumination*